LEVEL II

SDAC-TR-77-8

ON DETECTING AND ESTIMATING MULTIPLE ARRIVALS FROM UNDERGROUND NUCLEAR EXPLOSIONS

R.H. SHUMWAY & R.R. BLANDFORD

Seismic Data Analysis Center

Teledyne Geotech, 314 Montgomery Street, Alexandria Virginia 22314

25 MAY 1978

APPROVED FOR PUBLIC RELEASE; DISTRIBUTION UNLIMITED.

Sponsored by

The Defense Advanced Research Projects Agency (DARPA)

ARPA Order No. 2551

Monitored By

AFTAC/VSC

312 Montgomery Street, Alexandria, Virginia 22314

Disclaimer: Neither the Defense Advanced Research Projects Agency nor the Air Force Technical Applications Center will be responsible for information contained herein which has been supplied by other organizations or contractors, and this document is subject to later revision as may be necessary. The views and conclusions presented are those of the authors and should not be interpreted as necessarily representing the official policies, either expressed or implied, of the Defense Advanced Research Projects Agency, the Air Force Technical Applications Center, or the US Government.

Unclassified

SECURITY CLASSIFICATION OF THIS PAGE (When Data Entered)

REPORT DOCUMENTATION PAGE

READ INSTRUCTIONS BEFORE COMPLETING FORM

1. REPORT NUMBER: SDAC-TR-77-8	2. GOVT ACCESSION NO.
3. RECIPIENT'S CATALOG NUMBER	
4. TITLE (and Subtitle): ON DETECTING AND ESTIMATING MULTIPLE ARRIVALS FROM UNDERGROUND NUCLEAR EXPLOSIONS.	5. TYPE OF REPORT & PERIOD COVERED: Technical rept.
	6. PERFORMING ORG. REPORT NUMBER
7. AUTHOR(s): R. H. Shumway, R. R. Blandford	8. CONTRACT OR GRANT NUMBER(s): F08606-78-C-0007 w/ ARPA order-2551
9. PERFORMING ORGANIZATION NAME AND ADDRESS: Teledyne Geotech, 314 Montgomery Street, Alexandria, Virginia 22314	10. PROGRAM ELEMENT, PROJECT, TASK AREA & WORK UNIT NUMBERS: VT/8709 (12) 66
11. CONTROLLING OFFICE NAME AND ADDRESS: Defense Advanced Research Projects Agency, Nuclear Monitoring Research Office, 1400 Wilson Blvd. Arlington, Virginia 22209	12. REPORT DATE: 25 May 1978
	13. NUMBER OF PAGES: 63
14. MONITORING AGENCY NAME & ADDRESS (if different from Controlling Office): VELA Seismological Center, 312 Montgomery Street, Alexandria, Virginia 22314	15. SECURITY CLASS. (of this report): Unclassified
	15a. DECLASSIFICATION/DOWNGRADING SCHEDULE

16. DISTRIBUTION STATEMENT (of this Report)

APPROVED FOR PUBLIC RELEASE; DISTRIBUTION UNLIMITED.

17. DISTRIBUTION STATEMENT (of the abstract entered in Block 20, if different from Report)

18. SUPPLEMENTARY NOTES

Author's Report Date 07/14/77

19. KEY WORDS (Continue on reverse side if necessary and identify by block number)

Nuclear Explosion

Spall

pP

20. ABSTRACT (Continue on reverse side if necessary and identify by block number)

Nine explosions have been used to study the problem of specifying the number and characteristics of the arrival phases of a nuclear explosion. Tentative identification of the amplitudes and time delays of the multiple arrivals are given.

The method used is to scan the likelihood (L) for a single reflection model over amplitude (a) and time delay (t). The likelihood is constructed in the frequency domain using von Seggern and Blandford's (1972) source signal spectrum and a noise spectrum estimated from a time window preceding the signal.

DD FORM 1 JAN 73 1473 EDITION OF 1 NOV 65 IS OBSOLETE

Unclassified 408 258

SECURITY CLASSIFICATION OF THIS PAGE (When Data Entered)

The results demonstrated that pP was present along with additional multiple arrivals indicated by other peaks in the likelihood function, L. (Analysis extended to delays of 1.5 seconds, too short to detect spall except for PILEDRIVER, for which case it could not be detected.) In the case of MAST and PILEDRIVER, the likelihood estimate for τ was found to be clearly superior to $\tau = 1/f_n$, where f_n is the first null frequency. The result for PILEDRIVER, $\tau = .15$, is the first accurate estimate of τ for this event, and the shortest estimated delay time in the literature. The delay time for CANNIKIN, .55 sec, is significantly shorter than twice the observed uphole time: 1.0 sec. This result is unexplained, but it may be related to a change of reflection coefficient with frequency which is not included in the model. Comparison of theoretical and observed WWSSN long-period explosion P waves provides evidence for such a variable reflection coefficient.

Fair to good agreement was obtained between predicted and observed explosion periods measured on WWSSN long-period film and on LRSM short-period data which was deconvolved to appear as if recorded on the WWSSN long-period system.

A promising technique to determine yield and pP delay time given the WWSSN long-period amplitude and period is presented..

All these approaches require that both t* = travel-time/Q, and the reduced displacement potential as a function of depth and yield be known.

ON DETECTING AND ESTIMATING MULTIPLE ARRIVALS FROM UNDERGROUND NUCLEAR EXPLOSIONS

SEISMIC DATA ANALYSIS CENTER REPORT NO.: SDAC-TR-77-8

AFTAC Project Authorization No.:	VELA T/8709/B/ETR
Project Title:	Seismic Data Analysis Center
ARPA Order No.:	2551
Name of Contractor:	TELEDYNE GEOTECH
Contract No.:	F08606-78-C-0007
Date of Contract:	01 October 1977
Amount of Contract:	$2,674,245
Contract Expiration Date:	30 September 1978
Project Manager:	Robert R. Blandford (703) 836-3882

P. O. Box 334, Alexandria, Virginia 22313

ABSTRACT

Nine explosions have been used to study the problem of specifying the number and characteristics of the arrival phases of a nuclear explosion. Tentative identification of the amplitudes and time delays of the multiple arrivals are given.

The method used is to scan the likelihood ($\underline{L}$) for a single reflection model over amplitude (a) and time delay (τ). The likelihood is constructed in the frequency domain using von Seggern and Blandford's (1972) source signal spectrum and a noise spectrum estimated from a time window preceding the signal.

The results demonstrated that pP was present along with additional multiple arrivals indicated by other peaks in the likelihood function, $\underline{L}$. (Analysis extended to delays of 1.5 seconds, too short to detect spall except for PILEDRIVER, for which case it could not be detected.) In the case of MAST and PILEDRIVER, the likelihood estimate for τ was found to be clearly superior to $\tau = 1/f_n$, where f_n is the first null frequency. The result for PILEDRIVER, $\tau = .15$, is the first accurate estimate of τ for this event, and the shortest estimated delay time in the literature. The delay time for CANNIKIN, .55 sec, is significantly shorter than twice the observed uphole time: 1.0 sec. This result is unexplained, but it may be related to a change of reflection coefficient with frequency which is not included in the model. Comparison of theoretical and observed WWSSN long-period explosion P waves provides evidence for such a variable reflection coefficient.

Fair to good agreement was obtained between predicted and observed explosion periods measured on WWSSN long-period film and on LRSM short-period data which was deconvolved to appear as if recorded on the WWSSN long-period system.

A promising technique to determine yield and pP delay time given the WWSSN long-period amplitude and period is presented.

All these approaches require that both t* = travel-time/Q, and the reduced displacement potential as a function of depth and yield be known.

TABLE OF CONTENTS

LIST OF FIGURES

LIST OF FIGURES (Continued)

LIST OF TABLES

INTRODUCTION

Determining the P - pP delay poses an interesting problem during analysis of data generated by nuclear explosions. This delay can be used to provide an estimate for the depth of the event.

The model of interest is that the P-wave signal S_t will be seen on the seismometer as

$$Y_t = S_t + aS_{t-\tau} + n_t \qquad (1.1)$$

where τ is the delay time for pP and a is the relative amplitude for the reflected wave. The problems of estimating amplitude and the delay time usually depends upon noticing that for stationary and independently distributed signal and noise processes with spectra $P_s(f)$ and $P_n(f)$, respectively, the spectrum of observed data in (1.1) is given as

$$P_y(f) = |A(f)|^2 P_s(f) + P_n(f) \qquad (1.2)$$

where

$$A(f) = (1 + ae^{-2\pi i f \tau}) \qquad (1.3)$$

Here, we would have

$$|A(f)|^2 = 1 + a^2 + 2a \cos(2\pi f\tau) \qquad (1.4)$$

For a = -1 in Equation (1.4), as might be expected for pP, $P_y(f)$ will be zero for

$$f = \frac{m}{\tau}, \; m = 0, 1, \ldots\ldots$$

Cohen (1970), using detection of nulls, estimated the time delay as the reciprocal of the frequency for the first spectral null. Figure 1 shows the spectrum without nulls. Figure 2 shows the spectrum of the artificial time series

$$Y_t = 2(S_t - .5S_{t-.7}) + n_t$$

and we observe a first null at 1.56 Hz so that .64 seconds is the estimated delay time. The distortion due to the shape of the theoretical power spectrum of the signal $P_s(f)$, produced the discrepancy between 0.64 and 0.7 in this case. The normalized or "whitened" spectrum in which $P_s(f)$ is divided out showed a local minimum at .70 seconds. Cohen (1970) used this whitening method to determine pP and spall-created secondary phase P_s-P delays.

Cohen, T. J. (1970), Source-depth determination using spectral pseudo-autocorrelation and cepstral analysis, Geophys. J. R. Astr. Soc., 20, 223-231.

Another method of analysis (Bogert et al., 1962) is based upon the observation that for the noiseless case, the logarithm of the spectrum (1.2) is approximately, if a is small,

$$\log P_y(f) \approx \log P_s(f) + \log(1 + a^2 + 2a\cos 2\pi f\tau)$$

$$\approx \log P_s(f) + a^2 + 2a\cos 2\pi f\tau \qquad (1.5)$$

implying that the log spectrum is periodic. Thus, the spectrum of $\log P_y(f)$ should peak at $\tau = 1/f$. Ideally one would detrend by subtracting the log of the source spectrum as well as the overall mean. Cohen (1970) and Flinn et al. (1973) observed that for larger echo amplitudes ($|a| > .5$) the spectrum of the original spectrum produces a more pronounced peak than the spectrum of the log spectrum.

Bakun and Johnson (1973) fitted spectra (1.2) using least squares techniques to the CANNIKIN and MILROW events, identifying pP and spall phases along with the respective amplitudes and delay times. They also did the analysis in the time domain using homomorphic deconvolution to produce pulse wavelets corresponding to the different phases.

A natural extension of least squares fitting is to apply maximum likelihood in the frequency domain to develop estimators for the time delays and the amplitudes. Hannan and Thomson (1974) wrote the likelihood function assuming that the delay times and amplitudes are frequency dependent.

Bakun, W. H. and L. R. Johnson (1973). The deconvolution of teleseismic P waves from explosions MILROW and CANNIKIN, Geophys. J. R. Astr. Soc., 34, 321-342.

Bogert, B. P., Healy, M. J. R. and Tukey, J. W. (1962). The frequency analysis of time series for echoes: cepstrum, pseudo-autocovariance, cross sepstrum and phase cracking, in Proc. on Time Series Analysis, ed. M. Rosenblatt, John Wiley and Sons, New York.

Flinn, E. A., Cohen, T. J. and McCowan, D. W. (1973). Detection and analysis of multiple seismic events, Bull. Seis. Soc. Am., 63(6), 1921-1936.

Hannan, E. J. and Thomson, P. J. (1974). Estimating echo times, Technometrics, 16(1), p. 77-84.

However, they observed that frequency dependent estimators for these parameters tended to be about the same for each frequency. Estimators for the signal and noise spectra are made over narrow bands assuming that they are constant over the narrow bands and that $|A(f)|^2$ varies significantly over the same band. However, these assumptions are not reasonable for the seismic data considered here because in this study the authors assume in most cases that the source signal spectrum follows the model that von Seggern and Blandford (1972) described and that an independent estimator for noise spectrum can be derived from a time window preceding the signal. The approximate likelihood, then, can be written in terms of the delays and amplitudes over the whole frequency band of interest.

The basic data analyzed consists of nine selected explosions as recorded at several LRSM stations (Table I). The spectrum analyzed is determined as follows: Good signal-to-noise traces are selected. A cosine window is applied to the two seconds of noise preceding first motion, and another cosine taper is applied to the last five seconds of the records. Each of the traces is 12.8 seconds long. A 12.8 second noise sample in in front is identically tapered. The signal traces, preceded by their associated noise, are normalized by the maximum signal amplitude. To obtain the final "network" spectrum, the median of the signal spectra and of the noise spectra is calculated at each frequency.

---

von Seggern, D. and Blandford, R. (1972). Source time functions and spectra for underground nuclear explosions, Geophys. J. R. A. Soc., 31, 83-97.

TABLE I

Parameters of explosions considered in this paper, together with LRSM seismogram numbers and start points for the data used

	Depth (km) d	τpP Springer 1976	τ spall Springer 1976	τpP This Paper max-like	$\hat{v}$=2d/τpP Springer	$\hat{v}$=2d/τpP This Paper max-like	$\bar{v}$	LRSM Data Parameters (Station, Seismogram Number, Start Point) Z, R, T Components Used Except As Indicated
MILROW	1.22	.74	2.49	.85	3.3	2.9	4.1	KNUT 25893 5445 / RKON 25984 4672 / LCNM 25895 5030 / SJTX 25896 9619 (all 40 sps)
CANNIKIN	1.79	1.00	NA	.55*	3.6	6.6	4.4	PGBC 28302 5836 / KNUT 28303 3374 / RKON 28304 2489 / SJTX 28306 2578 / GATX 28307 4910
GREELEY	1.21	.97	NA	.70	2.5	3.5	3.5	PGBC 24318 1263 / RKON 24319 4767 / HNME 24321 1352 / KCMO 24323 1120 / NPNT 24325(R,T) 1828 / AX2AL 24327 1755
LONGSHOT	.70	.45	1.76	.55	3.1	2.6	3.2	RKON 25889 2899 / LCNM 25890 3891 / SJTX 25891 3723 / BEFL 25892(Z) 3530 (all 40 sps)
BUKARA (30 Sep 1966 05:59:52.8 38.8N, 64.5E, ISC)	2.45	-	-	1.20	-	4.1	3.0	NPNT 32205 3740 / RKON 32209 4000
EDAM	.41	-	.55	.55	-	1.5	1.6	RKON 30419 619
MAST	.91	-	.50*	.50*	-	3.6	3.9	HNME 30433 938 / RKON 30435 607 / WH2YK 30437 577 / FNWV 30441 566
MIZZEN	.64	-	.95	.95	-	1.4	1.5	RKON 30489 913 / WH2YK 30491 803 / FNWV 30495 695 / HNME 30497 785
PILEDRIVER	.46	.24	1.32	.15*	3.8	6.1	5.5	HNME 31507 2444 / NPNT 31509 2324 / PGBC 31511 720 / RKON(T) 31513 3340

* Not in agreement with first null

LIKELIHOOD FUNCTION

The model for the time series can be written as (1.1), leading to a model of the form (1.2), (1.3) for the spectrum. Suppose that an arbitrary signal gain factor θ is incorporated into the original equation yielding

$$Y_t = \theta(S_t + aS_{t-\tau}) + n_t \tag{2.1}$$

and

$$P_y(f) = \theta^2 \, |A(f)|^2 \, P_s(f) + P_n(f) \tag{2.2}$$

where

$$\begin{aligned} |A(f)|^2 &= |1 + ae^{-2\pi i f \tau}|^2 \\ &= 1 + a^2 + 2a\cos(2\pi f \tau) \end{aligned} \tag{2.3}$$

The signal spectrum $P_s(f)$ is derived from the von Seggern and Blandford (1972) model modified for the effects of the earth's absorption, that is

$$P_s^{1/2}(f) = \frac{(1 + (1+2B)^2 \, (\frac{2\pi f}{C})^2)^{1/2}}{(1 + (\frac{2\pi f}{C})^2)^{3/2}} \, e^{-\pi f t^*} I(f) \tag{2.4}$$

where I(f) is the instrument response, $t^* = T/Q$, where T is the travel-time, and Q the quality factor. The parameter C is related to yield Y in kilotons through the equation

$$C = k_o (Y/5)^{-1/3} \tag{2.5}$$

The observed spectrum is, then, a function of the parameters in the signal spectrum B, C, t^*, as well as the gain θ^2 and amplitude-time delay pair a, τ. While B is a non-dimensional parameter, C, k_o have the units of time.

Now, let $Y_T(f)$ be the FFT

$$Y_T(f) = T^{-1/2} \sum_{t=0}^{T-1} Y_t e^{-2\pi i f t} \tag{2.6}$$

so that an approximation to the joint log likelihood over L adjacent frequencies F_L which are integer multiples of $\frac{1}{T}$ can be written as

---

von Seggern, D. and Blandford, R. (1972). Source time functions and spectra for underground nuclear explosions, Geophys. J. R. Astr. Soc. 31, 83-97.

$$L(\theta^2, a, t, B, c, t^*)$$

$$= -L\log\pi - \sum_f \log P_Y(f) - \sum_f \frac{|Y_T(f)|^2}{P_Y(f)} \tag{2.7}$$

Assume first that parameters B, C, and t* can be determined reasonably well from site characteristics. An initial approximation to the maximum likelihood estimator for θ^2 is derived by setting the derivative of (2.7) equal to 0 and assuming that $P_n(f) \approx 0$. This procedure yields

$$\hat{\theta}^2 = \frac{1}{L} \sum_f \frac{|Y_T(f)|^2}{|A(f)|^2 P_s(f)} \tag{2.8}$$

where the solution depends upon the assumed values of a and τ. The likelihood (2.7) is then scanned, with $\hat{\theta}^2$ changing, over the values of a and τ restricted to a reasonable set, such as $-1 < a < 1$, .05 sec $\leq \tau \leq$ 2 sec. The range of f in (2.7) and (2.8) is 0.3 to 2.0 Hz in order to insure that only data with high values of S/N are considered. Note that $|Y_T(f)|^2$ is just the usual squared FFT or the sample periodogram.

In order to illustrate use of the likelihood function, artificial data was generated, conforming to the models

$$Y_t = 2S_t + n_t, \tag{2.9}$$

$$Y_t = 2(S_t - .5S_{t-.7}) + n_t \tag{2.10}$$

and

$$Y_t = 2(S_t - .5S_{t-.7} + .5\,[S_{t-.25} - .5S_{t-.95}]) + n_t \tag{2.11}$$

While the first equation has only a single arrival, (2.10) has a pP arrival at t = 0.7 seconds. Equation (2.11) has a pP arrival at 0.7 seconds and then a multipath of the complete signal .25 seconds later. In all cases we used B=2.0, C=7.6 (this corresponds to Y=10 kilotons in

granite) and t* = .55 as known parameters in the signal model (2.4). The theoretical process $P_n(f)$ was white and negligible.

Figure 1 shows the likelihood function under (2.9); note that it attains a maximum corresponding to a=0 in model (2.1) for any time delay, which leads to the single arrival explanation.

When the single reflection model (2.10) is introduced, the likelihood in Figure 2 shows a reasonably well defined peak at a = -.5 and τ = .7 seconds. One observed characteristic is that the time delay tends to be determined with higher resolution than the amplitude. Figure 2 shows that the observed and fitted spectrum agree very well.

The likelihood function even though it was designed for a single reflection model, can easily handle the more complicated double arrival defined by Equation (2.11). Figure 3 demonstrates that the theoretical spectrum of the data ($P_Y(f)$) shows no rippling for this signal spectrum. Thus, neither spectral analysis nor looking for nulls is expected to do well in this situation. Nevertheless, the two peaks in the likelihood correspond to the correct amplitudes and delay times. A narrowing of the main peak is the main impact on the signal spectrum.

The simulated examples seem to confirm that if the estimated source spectrum is correctly specified, then the multiple reflections can be sorted out even though they may not introduce any discernible periodicity in the observed spectrum. While the problem of independently estimating the B, C, and t* parameters, using the likelihood function, has not been considered in this initial study, it will be investigated in the following section for a number of nuclear explosions.

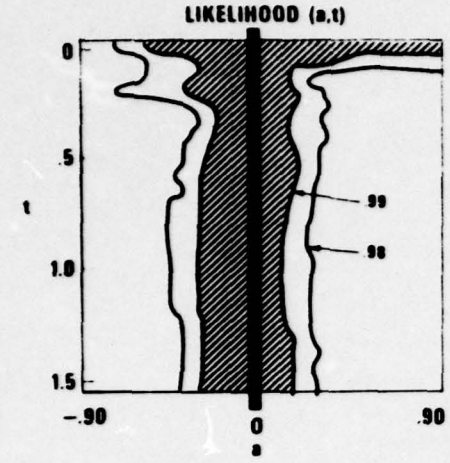

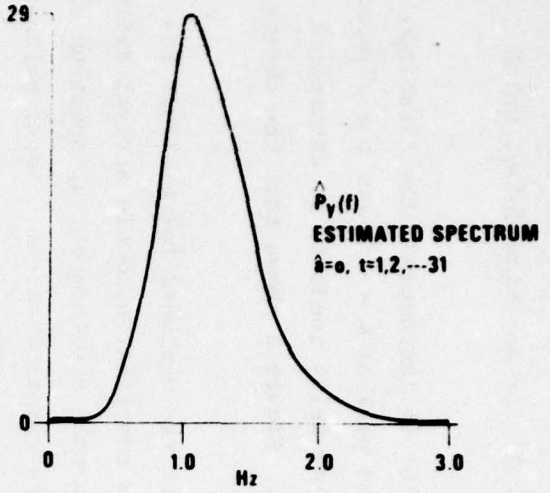

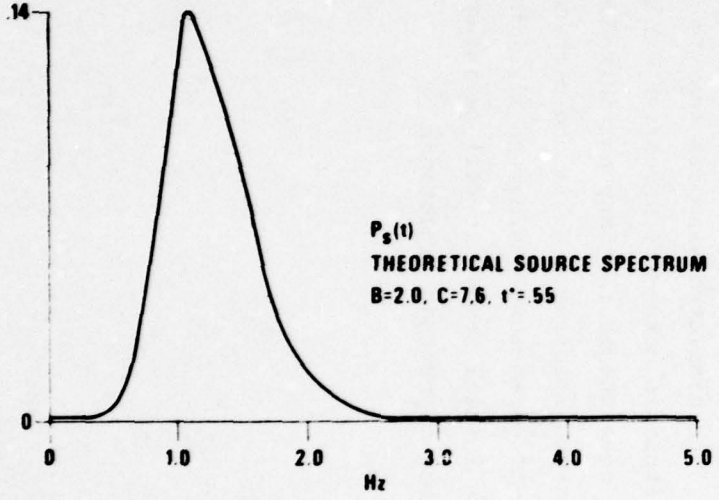

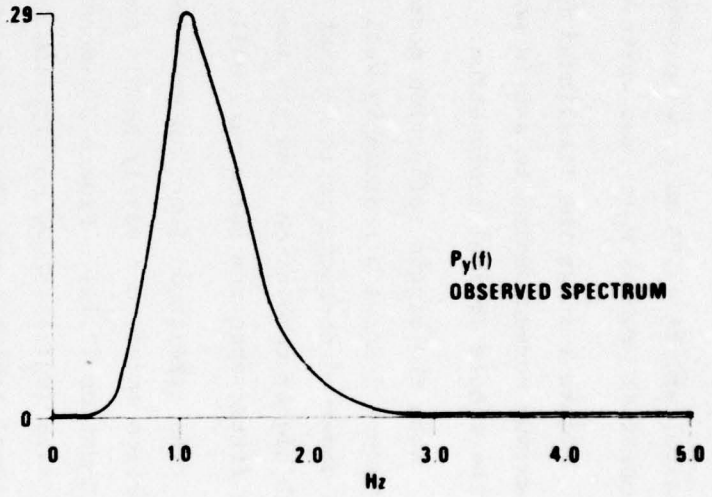

Figure 1. Analysis of artificial data generated according to the model $y_t = 2S_t + n_t$.

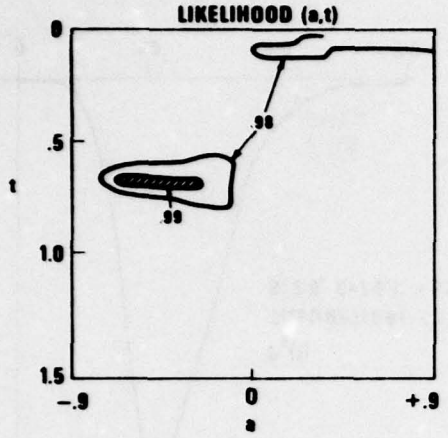

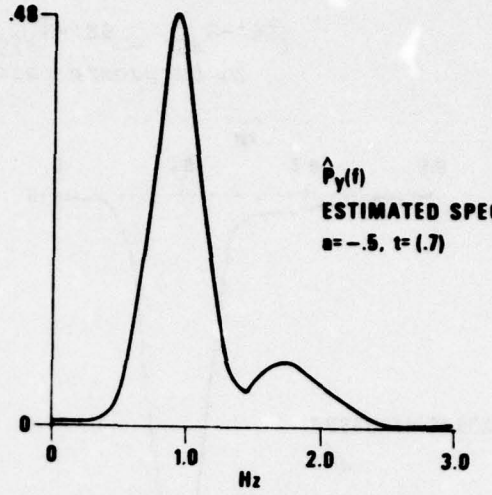

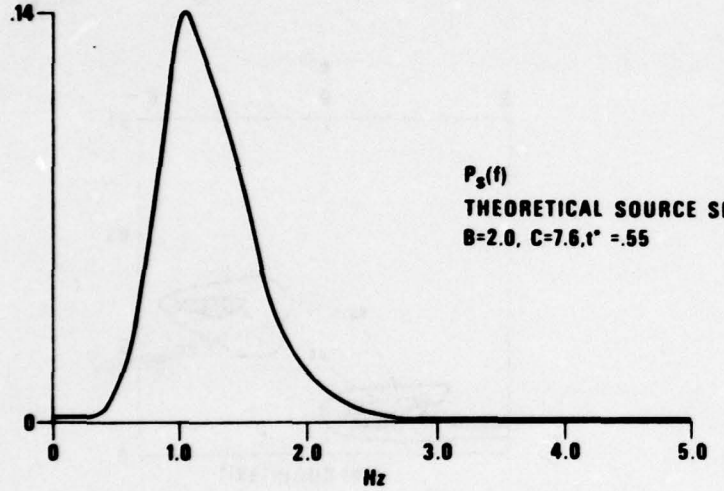

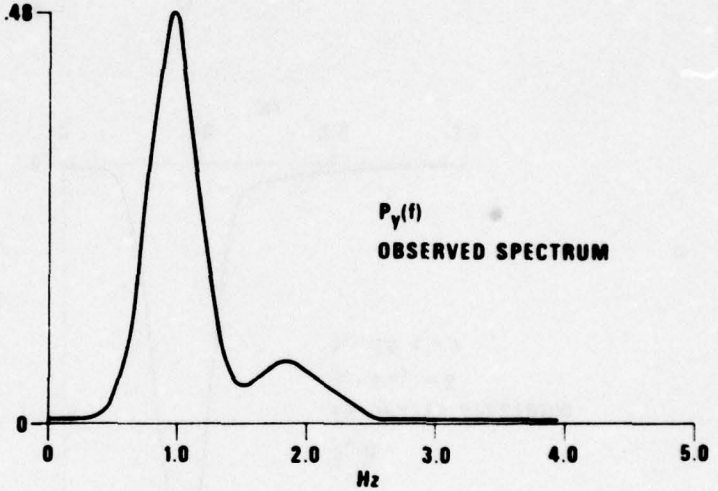

Figure 2. Analysis of artificial data generated according to the model $y_t = 2(S_t - .5S_{t-.7}) + n_t$.

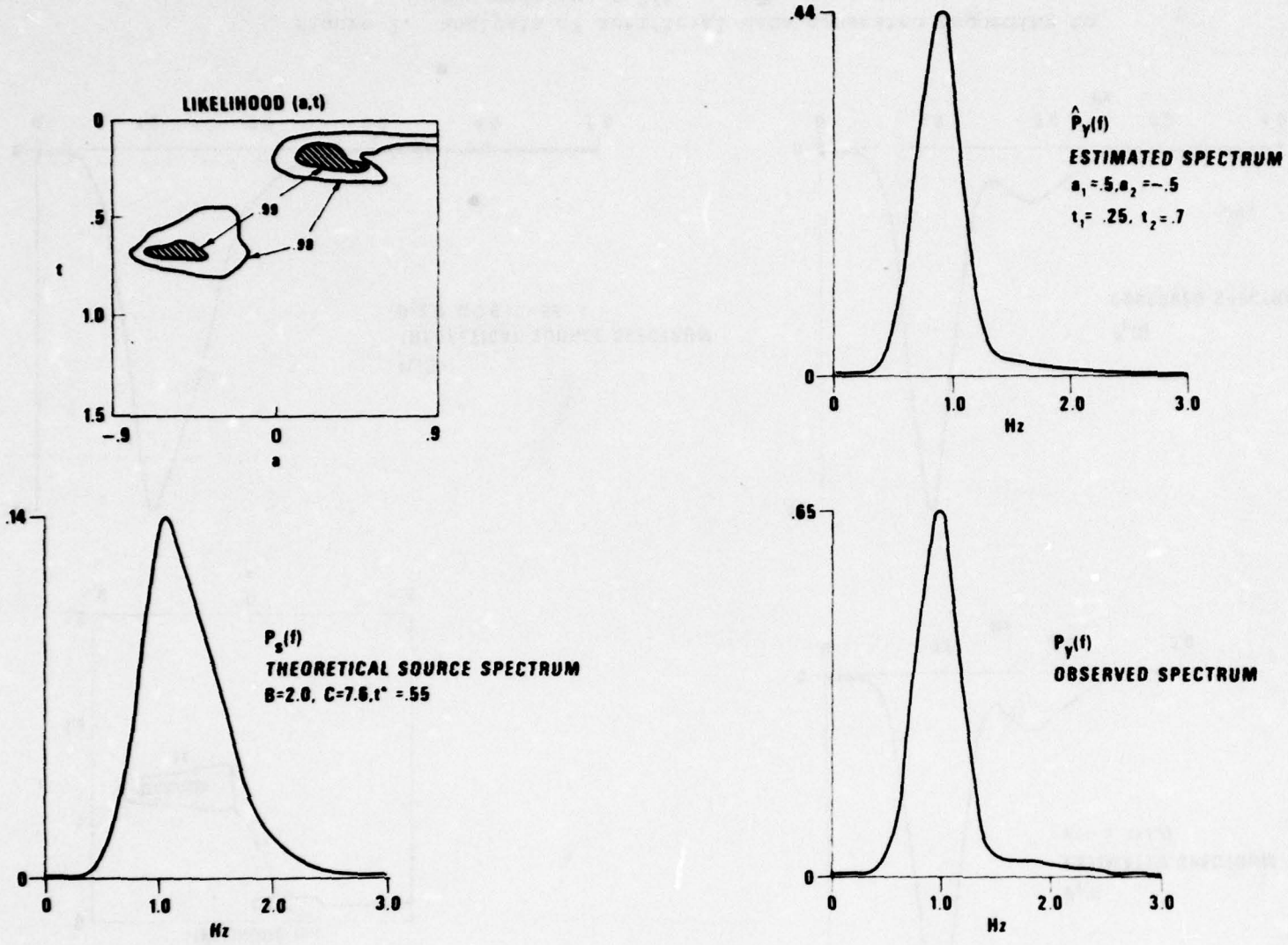

Figure 3. Analysis of artificial data generated according to the model $y_t = 2(S_t - .5S_{t-.7} + .5(S_{t-.25} - .5S_{t-.95}) + n_t$.

ESTIMATION OF pP DELAYS AND DEPTHS FOR NINE EXPLOSIONS USING LIKELIHOOD

Table I shows the nine explosions analyzed using the likelihood function along with information on depth and velocity in the overburden. The observed spectra are the median spectra from various combinations of LRSM stations as discussed earlier. Figures 4 through 12 display the likelihood functions, the observed spectra, and the fitted spectra corresponding to combinations of arrivals appropriate to sets of the observed maxima.

Table II summarizes estimated arrivals for each event with the arrivals selected as pP denoted by *. In most cases, pP is identified by looking for an arrival maximizing the likelihood and appearing with a negative amplitude.

For example, the peaks in the likelihood function indicate four arrivals corresponding to MILROW (Figure 4) with the third arrival maximizing the likelihood function at an amplitude of -.45 and time delay of .85 seconds. This delay is consistent with the first null observed at .80 seconds. An early poorly understood reflection (multipath?), which appeared at .25 seconds with a positive amplitude, showed frequently with these events. Theoretical spectra in Figure 4 are synthesized assuming two or four arrivals with the delay times and amplitudes indicated. The two-arrival model appears to yield a better fit for this particular case. In principal, each positive amplitude arrival (multipath) could have a corresponding negative amplitude for pP. However, these amplitudes would be small and they have been neglected in the reconstructions.

In each case except BUKARA which was detonated in clay (Marshall, 1972), the scaled granite source model of von Seggern and Blandford was used. An attempt to match the overall spectral shape of BUKARA by visual matching of observed and theoretical spectra led to the source spectral values B=0, C=4.0. Matching the high frequency (2-5 Hz) slopes of the median spectra with good signal-to-noise ratios led to t* values of .55 for NTS explosions, and .27 for Amchitka explosions. These should be regarded as "median" t* values suitable for the "median" spectrum.

Marshall, P. D., (1972). Some seismic results from a world wide sample of large underground explosions, AWRE Report O 49/72, Atomic Weapons Research Establishment, Aldermaston, Berkshire, United Kingdom.

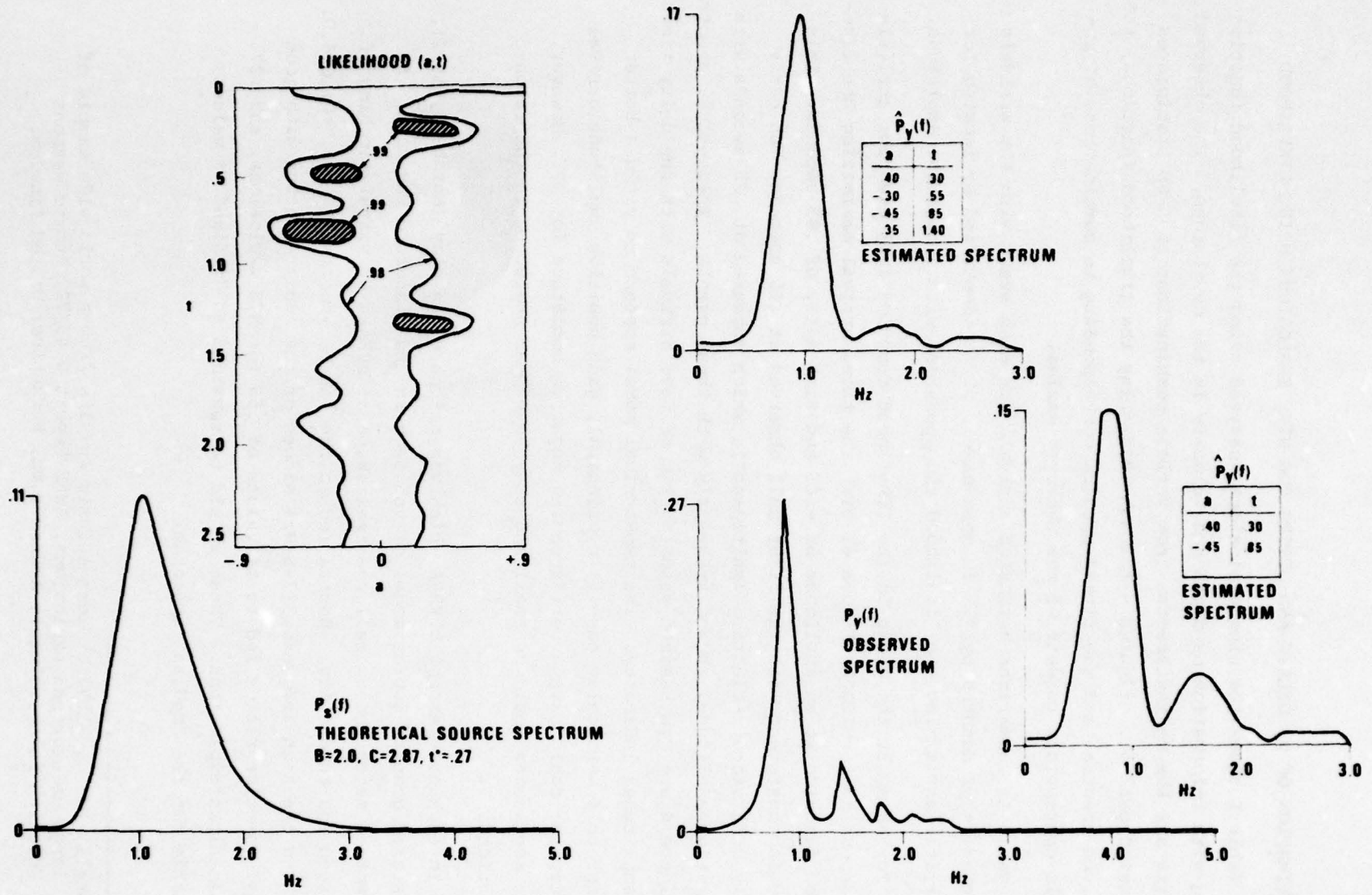

a	t
40	30
-30	55
-45	85
35	140

a	t
40	30
-45	85

Figure 4. Analysis of MILROW event showing pP at 0.85 sec.

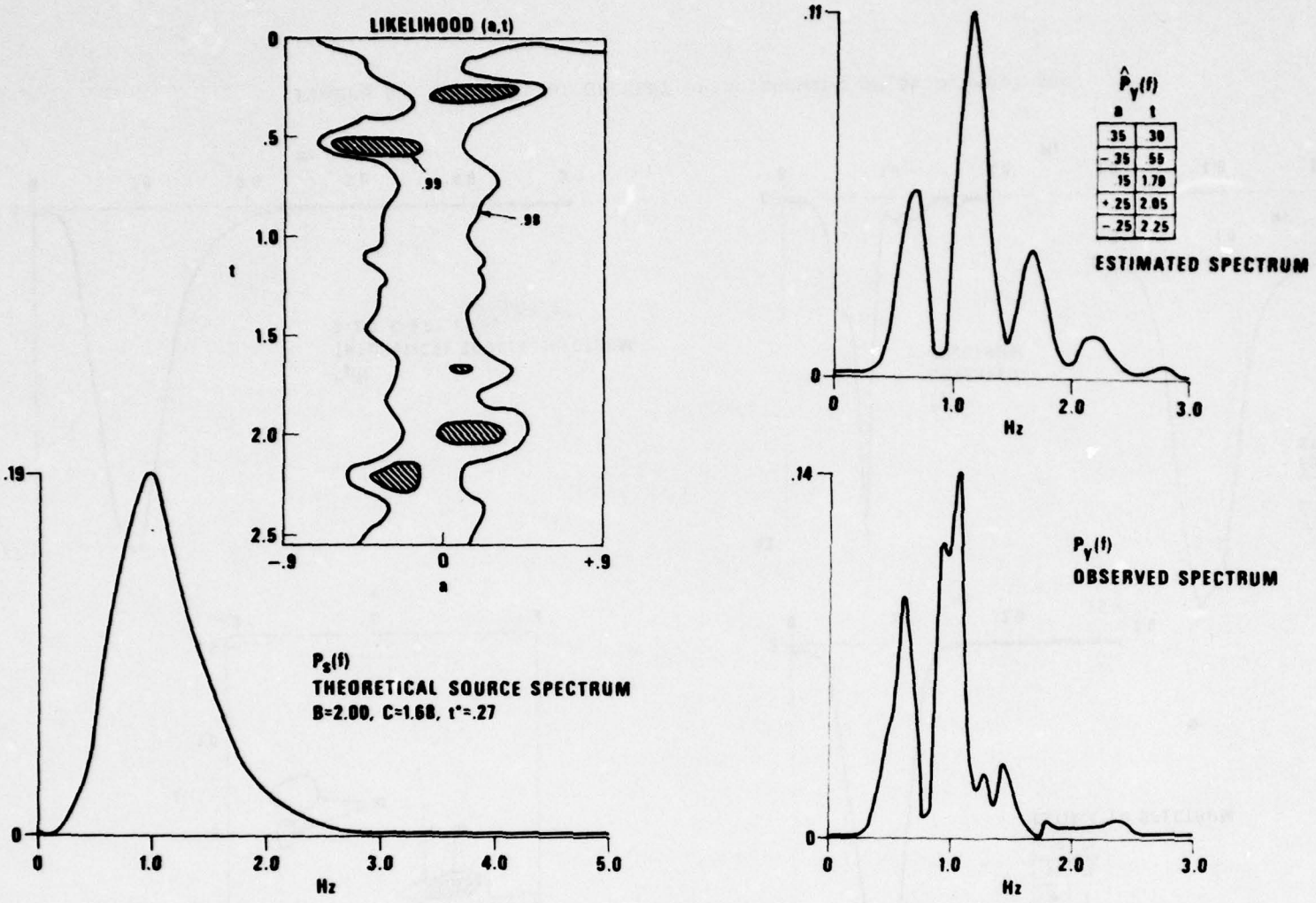

Figure 5. Analysis of CANNIKIN event showing pP at 0.55 sec.

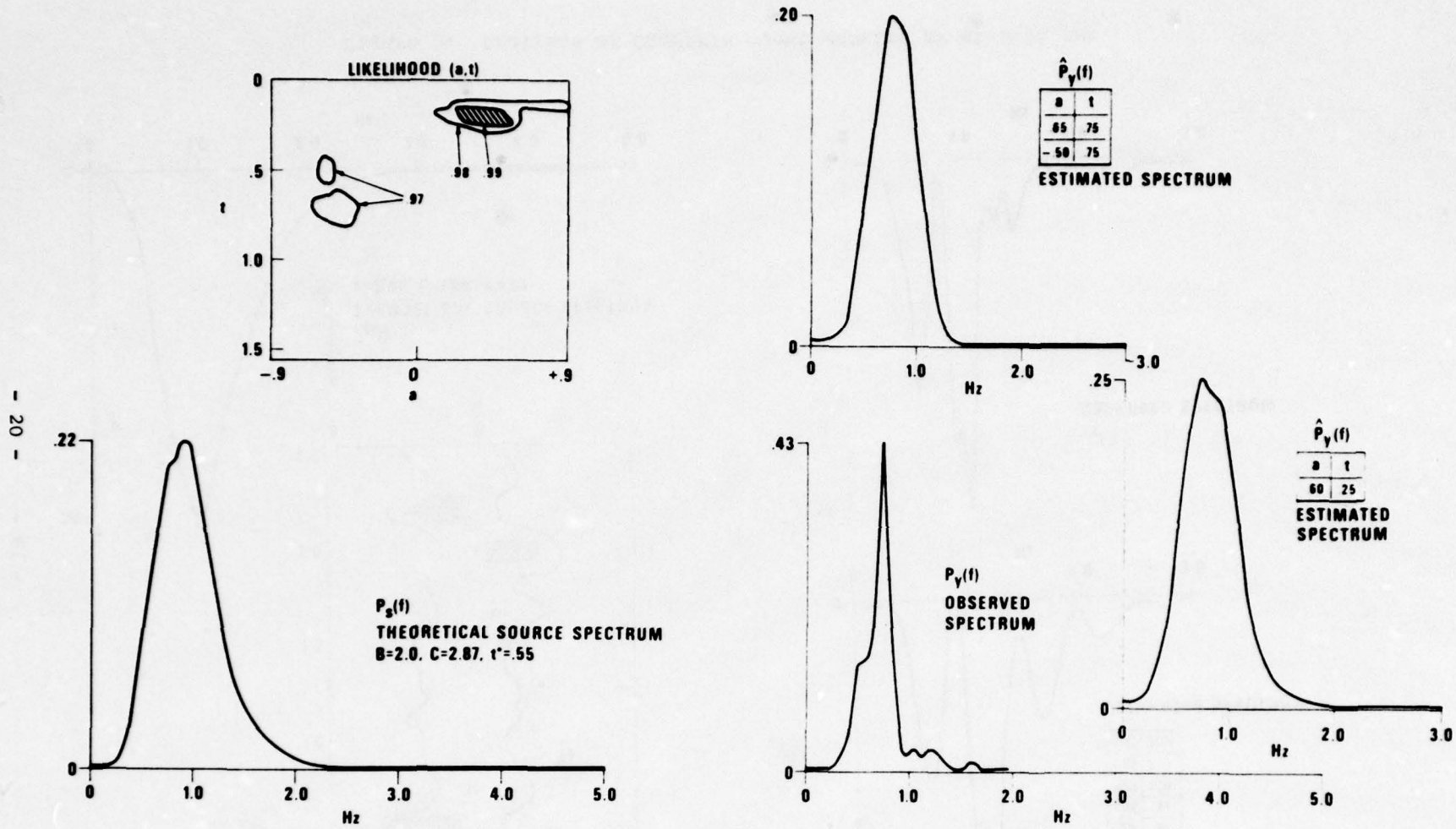

Figure 6. Analysis of GREELEY event showing pP at 0.5-0.7 sec.

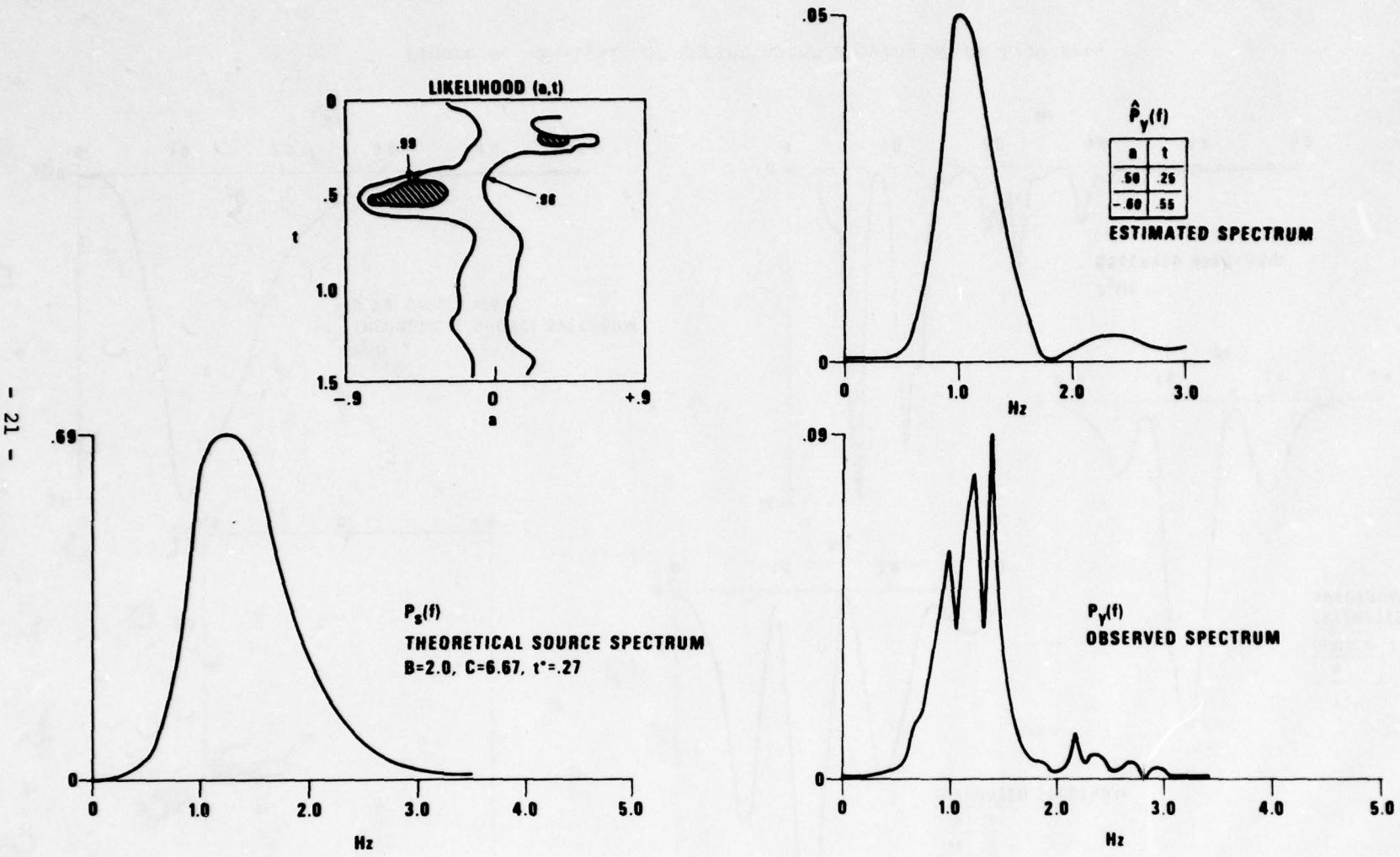

Figure 7. Analysis of LONGSHOT event showing pP at 0.55 sec.

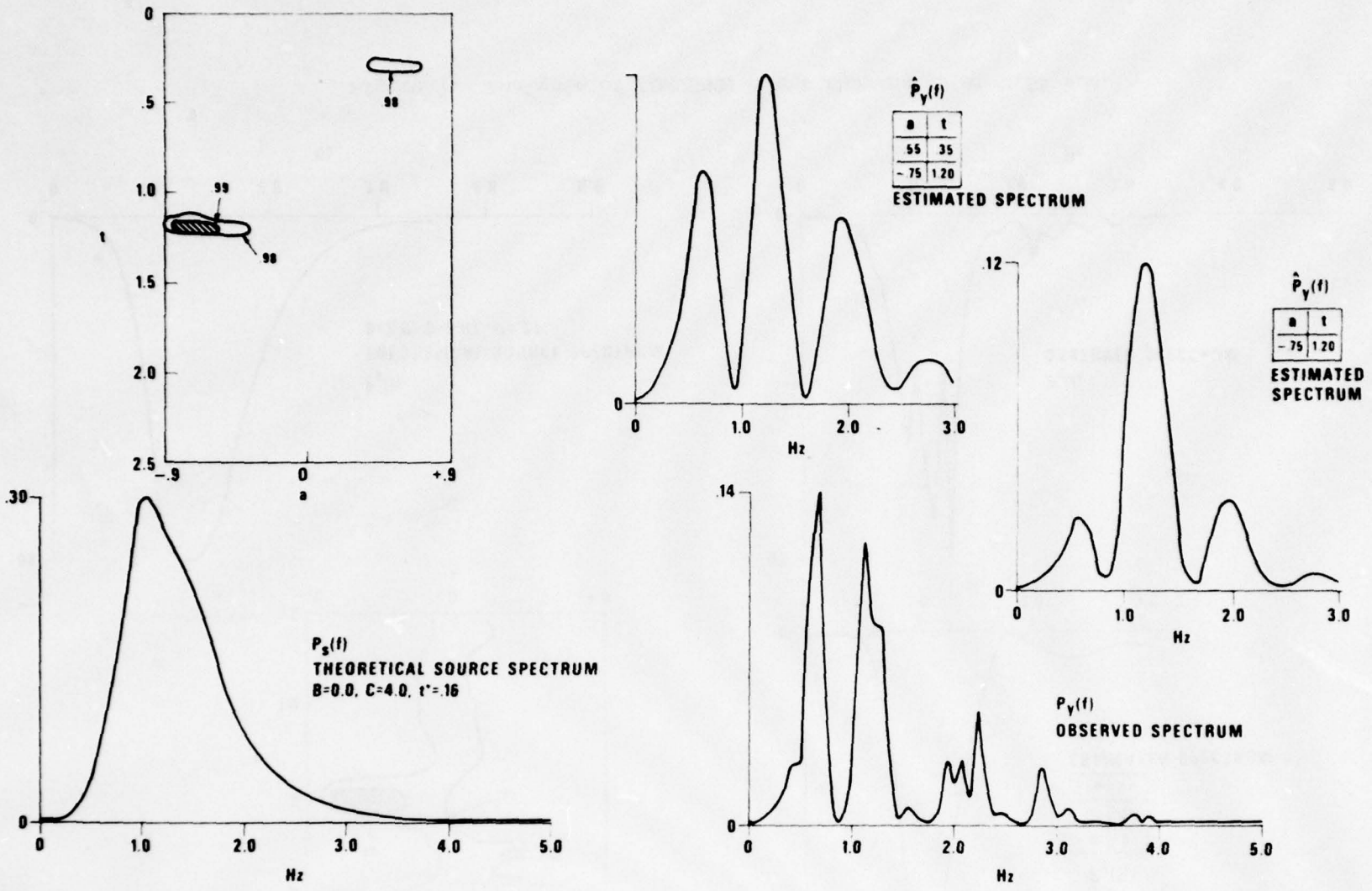

Figure 8. Analysis of BUKARA event showing pP at 1.20 sec.

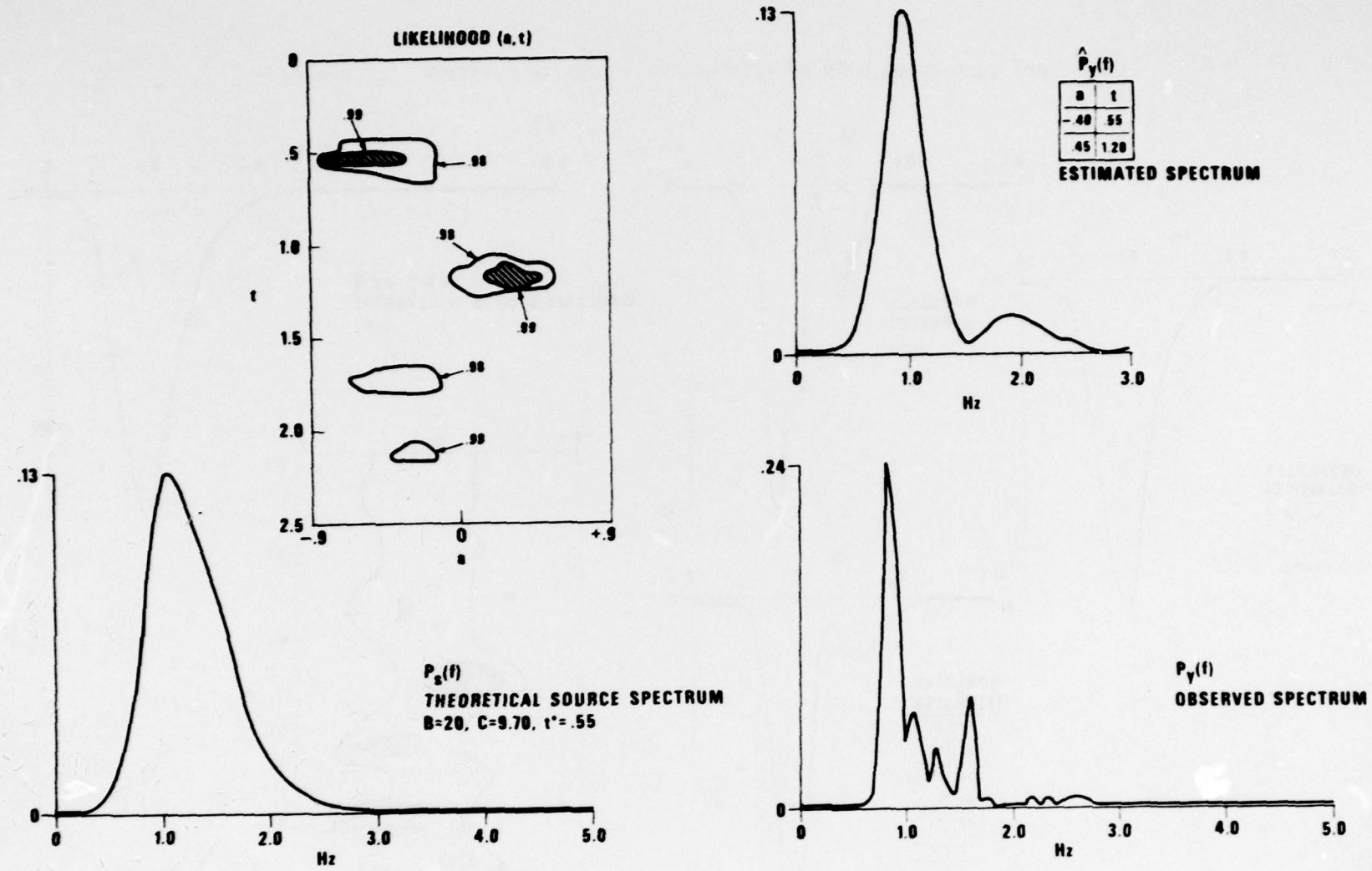

Figure 9. Analysis of EDAM event showing pP at 0.55 sec.

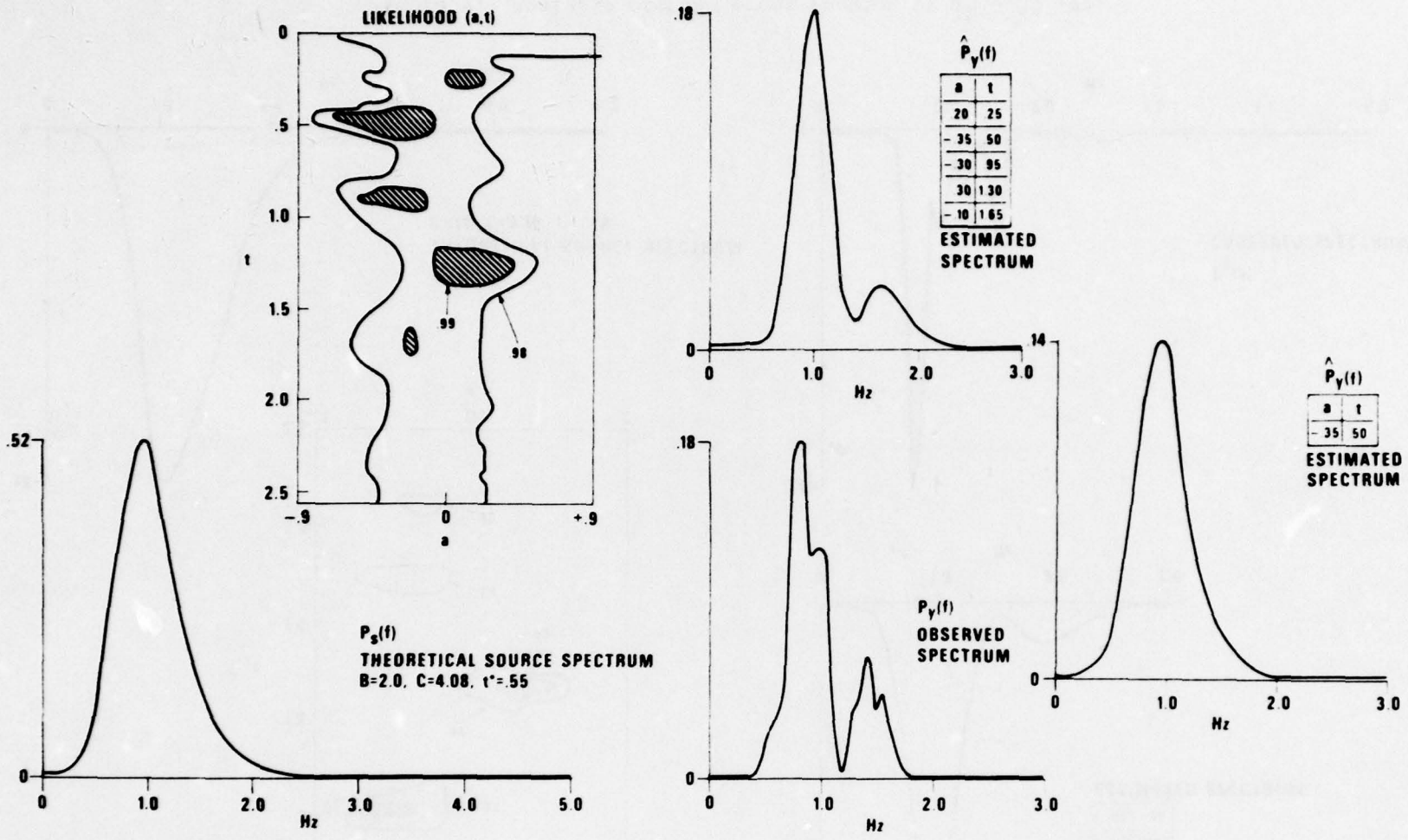

Figure 10. Analysis of MAST event showing pP at 0.50 or 0.95 sec.

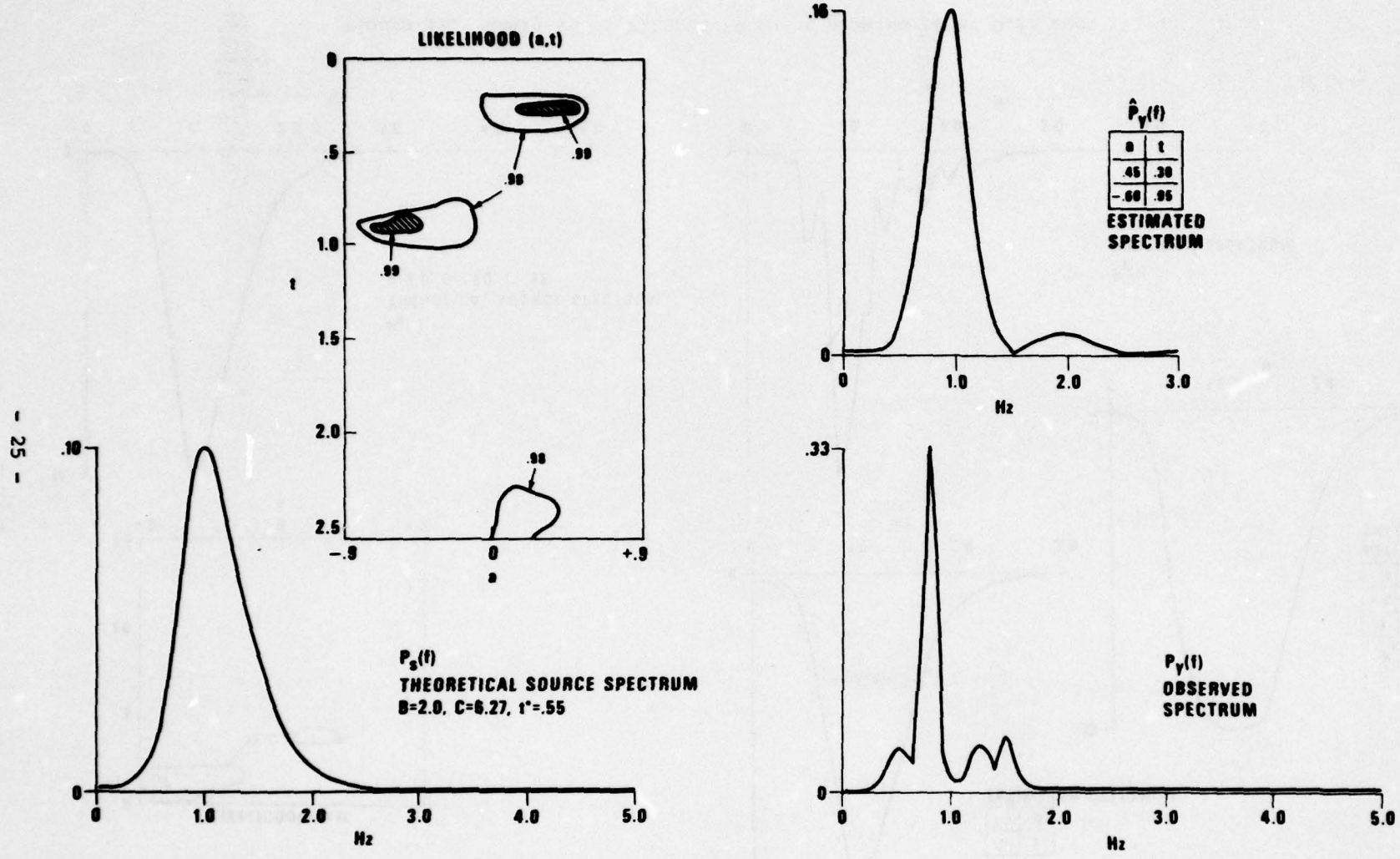

Figure 11. Analysis of MIZZEN event showing pP at .95 sec.

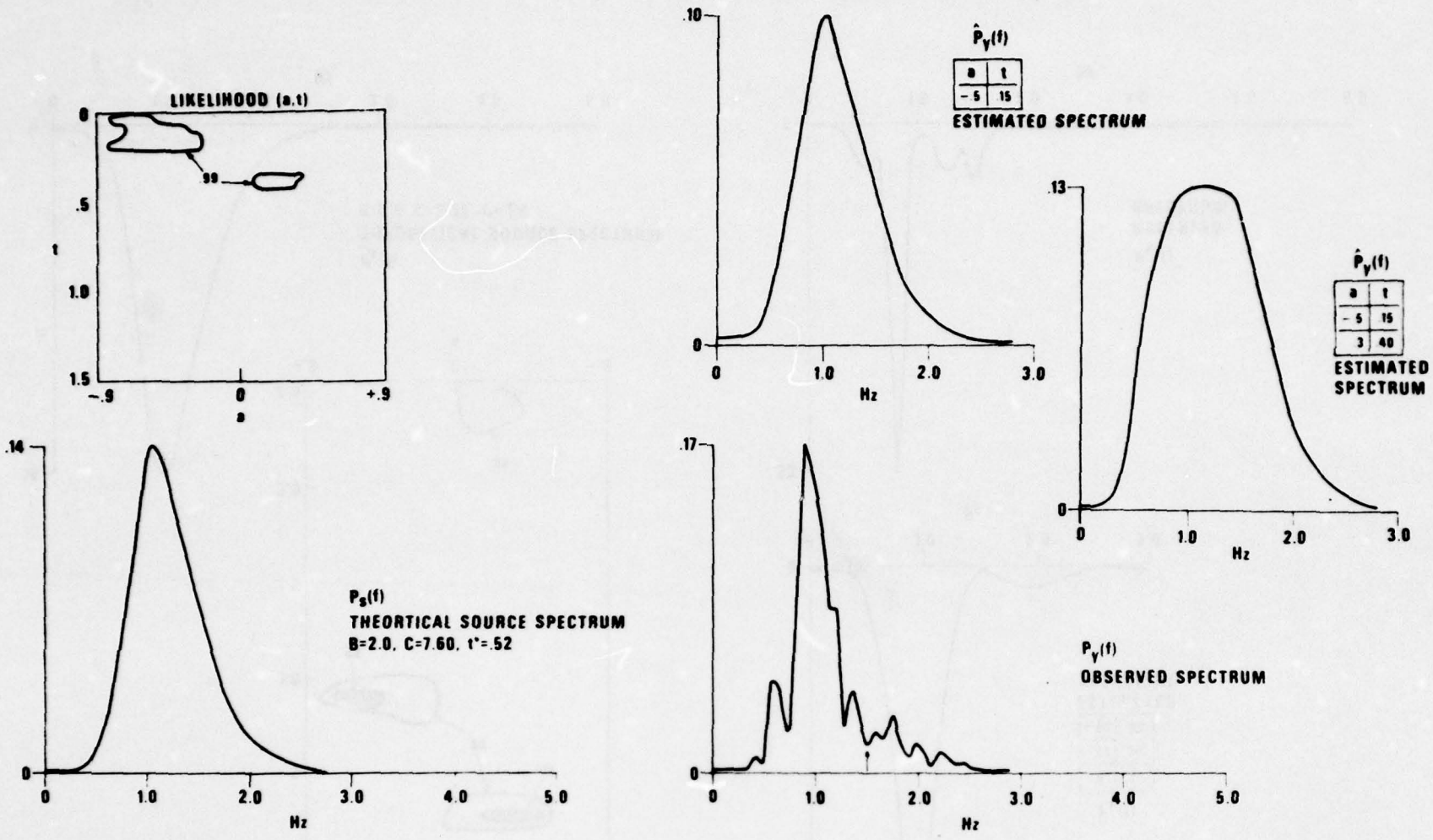

Figure 12. Analysis of PILEDRIVER event showing pP at 0.15 sec.

TABLE II

Parameters of maximum-likelihood estimated arrival phases for a suite of explosions, together with the B, C, and t* values assumed

			a	T	L	B	C	t*
1.	MILROW	1	.40	.30	1.377	2.00	2.87	.27
	Estimated from	2	-.30	.55	1.369			
	first null τ =	*3	-.45	.85	1.378			
	(.80)	4	.35	1.40	1.374			
2.	CANNIKIN	1	.35	.30	1.428	2.00	1.68	.27
	Estimated from	*2	-.35	.55	1.429			
	first null τ =	3	.15	1.70	1.415			
	(1.16)	4	-.25	2.05	1.422			
		5	-.25	2.25	1.422			
3.	GREELEY	1	.60	.25	1.771	2.00	2.87	.55
	No visible	2	-.45	.50	1.701			
	null	*3	-.55	.70	1.712			
4.	LONGSHOT	1	.50	.25	1.440	2.00	6.67	.27
	Estimated from	*2	-.60	.55	1.450			
	first null τ =							
	(.51)							
5.	BUKARA	1	.55	.35	--	0.00	4.00	.16
	Estimated from	*2	-.75	1.20	1.314			
	first null τ =							
	(1.07)							
6.	EDAM	*1	-.40	.55	1.487	2.00	(k_o=16.8)	.55
	Estimated from	2	.45	1.20	1.486			
	first null τ =							
	(.67)							
7.	MAST	1	.20	.25	1.551	2.00	(k_o=16.8)	.55
	Estimated from	*2	-.35	.50	1.564			
	first null τ =	3	-.30	.95	1.554			
	(.80)	4	.30	1.30	1.562			
		5	-.10	1.65	1.549			
8.	MIZZEN	1	.45	.30	1.463	2.00	(k_o=16.8)	.55
	Estimated from	*2	-.60	.95	1.453			
	first null τ =							
	(.91)							
9.	PILEDRIVER	*1	-.5	.15	1.437	2.00	7.60	.55
	Estimated from	2	.3	.40	1.434			
	first null τ =							
	(.64)?							

* Phase selected for pP

A computation for the apparent depth can be made using $d = \bar{v}\,\tau/2$ or for the predicted delay by $\hat{\tau} = 2(d/\bar{v})$ where $\bar{v}$ is the shot-point to surface average velocity of the overburden (Table I) and τ is the estimated pP time delay. Figure 13 shows the depths computed from the likelihood approach compared with published depths for the nine events.

Below, the events are discussed separately:

MILROW (Figure 4)

The MILROW results are in good agreement with Bakun et al's (1973) earlier results and with the pP estimates from Springer's (1974) shot point recordings. Depths estimated from the first null and from maximum likelihood are comparable.

CANNIKIN (Figure 5)

For CANNIKIN achieving good agreement is possible with the observed spectrum with a suite of five arrivals, including one with negative amplitude and with maximum likelihood at 0.55 seconds delay. Springer (1974) obtained 1.0 seconds for pP, and Bakun and Johnson (1973) obtained 1.5 seconds. Consideration of the first null leads to an estimated delay of 1.16 seconds. Clearly, our result disagrees with previous work. Use of delays and amplitudes proposed by Bakun and Johnson, which include a multipath, results in a theoretical spectrum that is not as good a match to our observed spectraum as the theoretical spectrum determined in this report. Adjustments of t* have been attempted, but they did not yield a maximum likelihood estimate for a negative delay near 1.0 second. This result suggests a failure of the maximum-likelihood technique. One explanation for this outcome is that because of the large yield, the spectrum is heavily shifted to lower frequencies where the reflection coefficient is rapidly changing from about 1.0 to some smaller absolute value, representing a failure of the model. This matter is discussed in more detail in the following sections.

Bakun, W. H. and L. R. Johnson, 1973, The deconvolution of teleseismic P waves from explosions MILROW and CANNIKIN; Geophys. J. R., 34, 321-342.

Springer, D. L., 1974, Secondary sources of seismic waves from underground nuclear explosions; Bull. Seism. Soc. Am., 64, 581-594.

GREELEY (Figure 6)

Analysis of GREELEY gives an accurate result despite absence of a prominent spectral null. In this case the maximum-likelihood technique is clearly superior to standard methods. Note, however, that the theoretical maximum-likelihood spectrum is broader than the observed spectrum and that the absolute maximum of the likelihood function occurs for the multiple and not for pP. Note that in CANNIKIN, MILROW, and now GREELEY there has been a small positive multiple around 0.3 seconds. Experiments with artificial data show that the maximum-likelihood technique is unable to distinguish between a precursor and a later arrival which have the same absolute delay relative to the largest arrival. (Eliminating this ambiguity is a subject for future research.) Therefore, this multiple can be interpreted as a precursor, explaining the small first motions observed at most stations for these and most other explosions.

LONGSHOT (Figure 7)

For LONGSHOT agreement between theoretically calculated spectrum and observed spectrum is good. A precursor is evident and the pP delay is in good agreement with results from earlier workers and with the first null seen in Tables I and II.

BUKARA (Figure 8)

The event at BUKARA is different from others in this study because B and k_o had to be estimated from the data. The standard granite potential, together with the yield given by Marshall (1972) of approximately 30 kt, proved unable to reasonably match the observed spectrum with any of a complete range of t* values. Marshall (1972) stated that this event was detonated in clay, a medium very much different from granite. One might intuitively expect little overshoot, a long time-constant, and low attenaution from this shot as recorded at NPNT. By trial and error a good fit was found to the spectral envelope for B=0, k = 7.3, and t* = 0.16. These parameters yielded a good match to the complete modulated spectrum yielding a delay time in good agreement with Marshall's (1972) deconvolution results and with simple first null considerations. This event, with its large delay and good high-frequency data is easy to analyze. The estimated reflection coefficient is -0.75, the

largest ever reported. This coefficient could result from the (1) less rugged surface topography than at other deep shot sites such as NTS and Amchitka, (2) from the fact that a small shot, being overburied, has not crushed and distorted as much of the medium as larger shots, (3) that less of the pP energy has gone into spall since the reflected wave of dilatation may be too weak to create substantial spall because the surface is far from the detonation point.

EDAM (Figure 9)

In this case good agreement is also obtained between predicted and observed delay times. This shot is interesting because it is relatively small, detonated at Yucca in a very low velocity medium, and analyzed only at RKON. Approximately the same delay would be obtained by first null considerations.

MAST (Figure 10)

This event shows a complicated pattern of relatively weak arrivals, which, taken together, match the observed spectrum well. The strongest arrival of opposite polarity gives a delay of 0.5 seconds, in good agreement with the predicted delay. However, another weaker "reflection" with 0.95 delay exists that is in fair agreement with the delay which would be predicted from first null considerations of 0.8 seconds. In this case a clear first null gives a significantly incorrect result.

MIZZEN (Figure 11)

Here is a simple case where the predicted delay time is in good agreement with the maximum-likelihood estimate and with first null analysis.

PILEDRIVER (Figure 12)

For this event good agreement exists between the predicted and observed pP delay time of $2 \times (0.46/5.5) = 0.17$ and 0.15 seconds, respectively. In fact, the maximum likelihood estimate is in better agreement with the predicted value than the spall-derived time of 0.24 seconds that Springer (1974) presented. Although in this case no clear first null exists, a suggestion of

---

Springer, D. L., 1974, Secondary sources of seismic waves from underground nuclear explosions, Bull. Seism. Soc. Am., 64, 581-594.

one is evident yielding an incorrect delay of 0.64 seconds. In Figure 13 are summarized the foregoing results in a comparison of known depths as compared to depths calculated using known velocities and the maximum likelihood estimates of τ. We note that the the depth estimate using Springer's (1974) τ estimate has the same size error as the depth estimate from this paper. The medium velocity for BUKARA is uncertain.

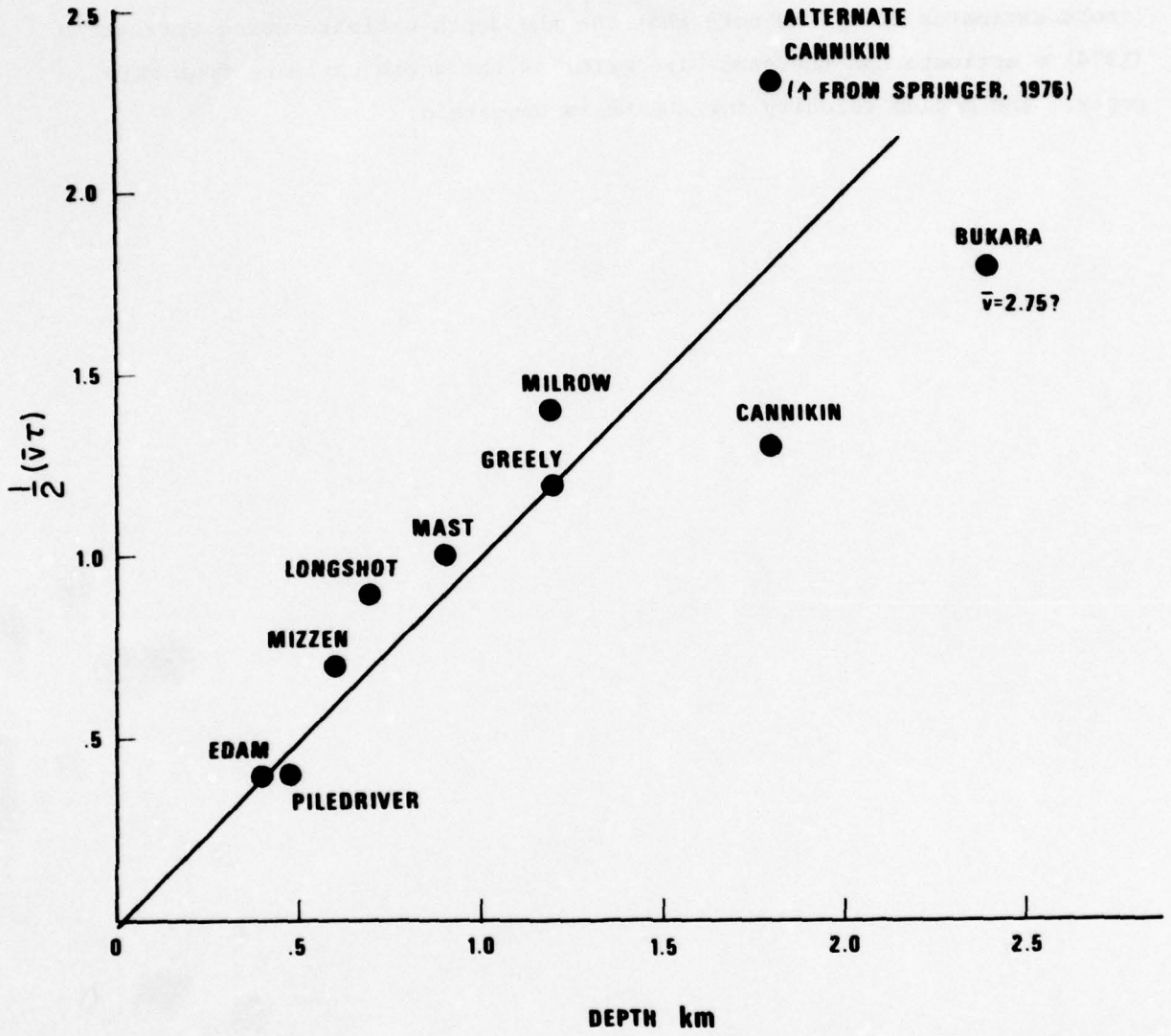

Figure 13. Depth estimated from in-situ uphole average velocity divided by delay time estimated from the maximum likelihood technique plotted as a function of known depth.

IMPLICATIONS OF WWSSN LONG-RANGE RECORDINGS OF LARGE-EXPLOSION P WAVES

Figure 14a shows WWSSN long-period recordings of CANNIKIN. Twice the peak-to-trough time can be estimated to be 3.2 seconds, with some care on the good signal-to-noise traces. In Figure 14b, WWSSN long-period recordings of P waves from a nearby earthquake show typical earthquake periods of 10 seconds. Note also that although the CANNIKIN m_b is a full magnitude larger than that of the earthquake, the long-period amplitude is only 2 to 3 times larger. Together, these facts show that proportionally less long-period energy is emitted from the CANNIKIN epicenter than from the earthquake. For CANNIKIN, 0.8 Hz is the frequency where the amplitude spectrum of scaled granite-reduced displacement potential falls to one-half of the low-frequency limit. A peak in the theoretical spectrum occurs at about 3-second period. The magnitude 6.1 earthquake might well have a corner frequency lower than 0.3 to 0.8 Hz. If so, this alone might account for the difference in the observed frequency content of the signals. However, the granite-reduced displacement potential is not compatible with observed CANNIKIN waveforms, unless the pP phase cancels much of the low-frequency signal. Without pP, the explosion waveform would be predicted to show periods similar to those of the Amchitka earthquake. Thus, perhaps pP is basically responsible for the difference in signal period between CANNIKIN and the earthquake.

Figures 15a and 15b show signals from JORUM at NTS and from the nearby San Fernando earthquake of comparable m_b. Again, the long-period P-wave signals for the explosion are of higher frequency and are 10 to 20 smaller in amplitude. The granite potential for JORUM places the one-half amplitude point for the spectrum at 1.4 Hz, and the spectral peak at 1.7 sec. According to Wyss and Hanks (1972), the corner frequency for the San Fernando earthquake is approximately 0.15 Hz, again showing that the difference in source-spectra alone is sufficient to qualitatively explain the difference between the long-period signals. However, quantitatively we shall see that we require the effect of pP to reduce the theoretical period expected from underground

---

Wyss, M. and T. C. Hanks, 1972. The source parameters of the San Fernando earthquake inferred from teleseismic body waves, Bull. Seism. Soc. Am., 62, 591-602.

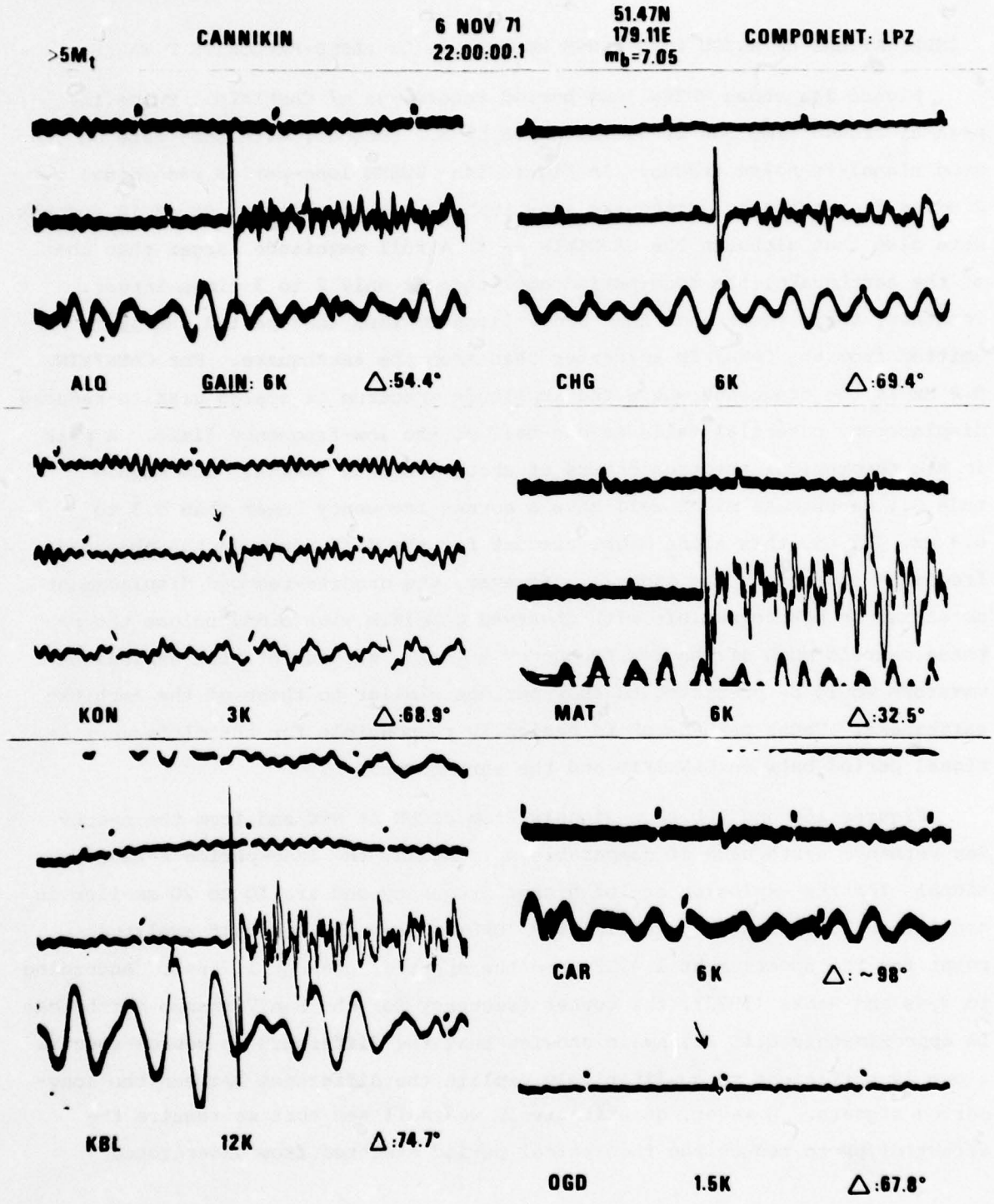

Figure 14a. WWSSN long-period recordings of P from CANNIKIN. Gains as printed are 1.63 times those indicated on the figure which are those given on the original film.

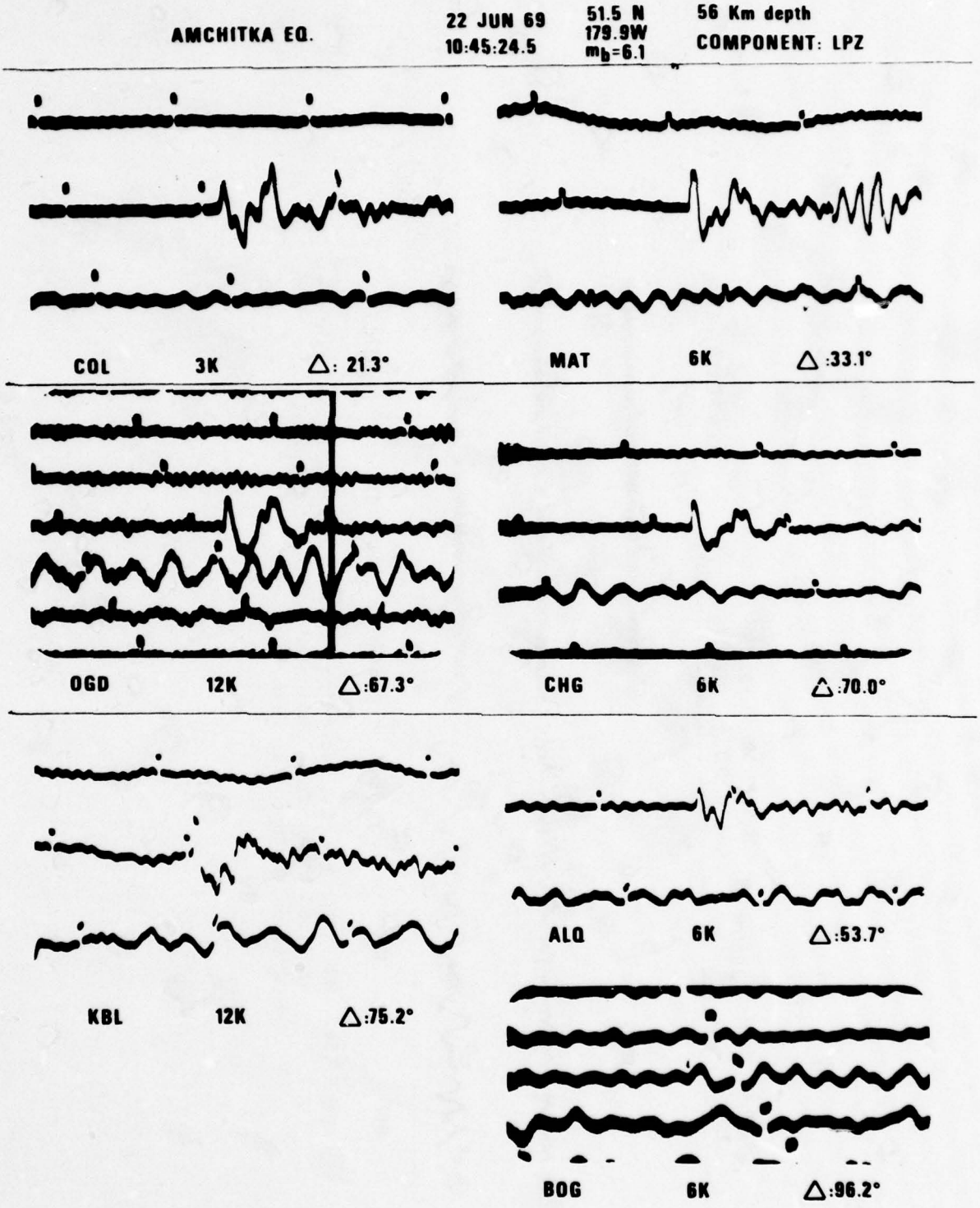

Figure 14b. WWSSN long-period recordings from the Amchitka earthquake of 22 June 1969. Gains as printed are 1.63 times those indicated on the figure which are those given on the original film.

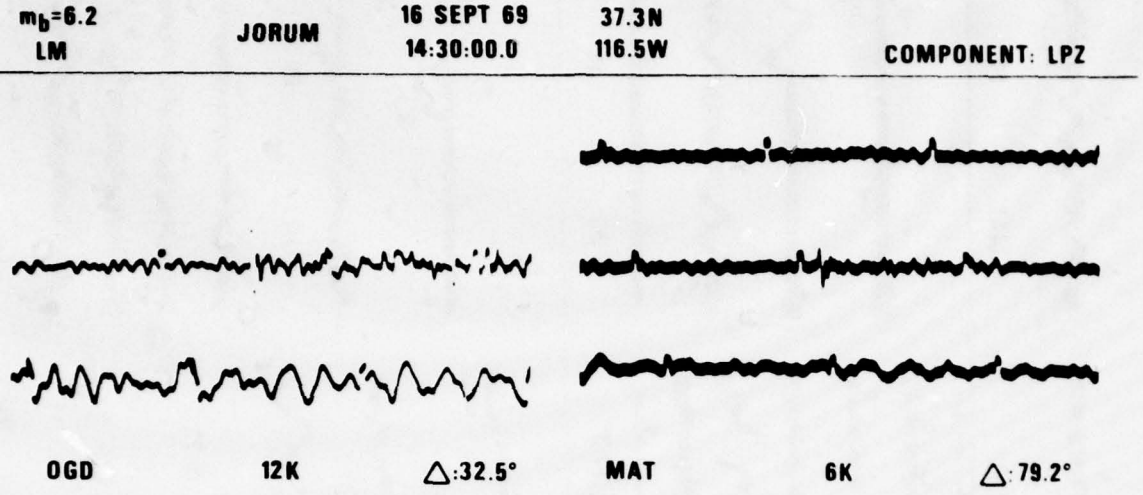

Figure 15a. WWSSN long-period recordings from JORUM. Gains as printed are 1.63 times those indicated on the figure which are those given on the original film.

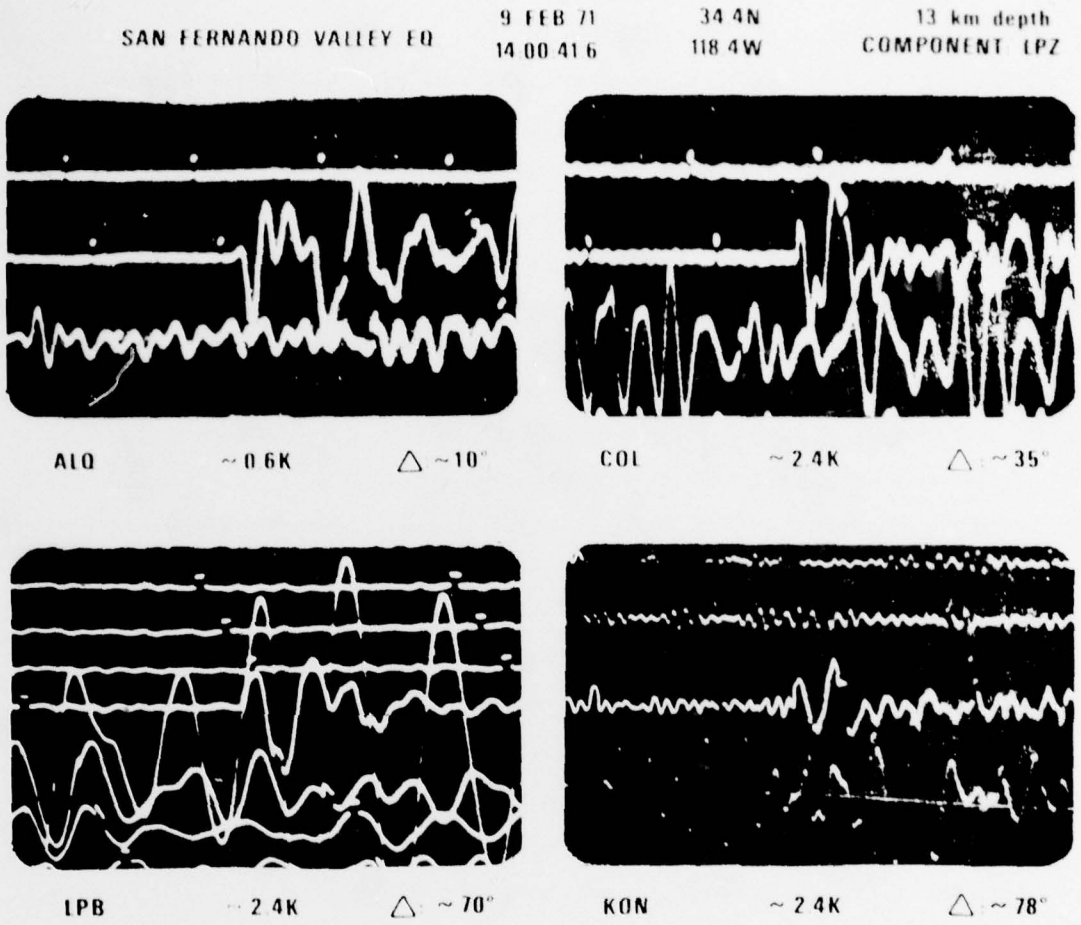

Figure 15b. WWSSN long-period recordings from the San Fernando earthquake, 9 February 1971. Gains as printed are 1.63 times those indicated on the figure which are those given on the original film.

explosions to be in agreement with observed values.

Figures 16a,b,c show theoretical WWSSN long-period waveforms for a range of yields from 20 to 5000 kt and for t* = .25, and .5. The delay times for pP are given by formula $\tau = \tau_o Y^{1/3}$ seconds with Y in kilotons. Calculations are given for no pP and with τ_o = 0.03, 0.05, 0.1, 0.15, 0.2. τ_o = 0.03 corresponds to an underburied shot in granite (a shallower PILEDRIVER), 0.20 could correspond to shots in some of the very low velocity sediments at Yucca Flats, such as EDAM or MIZZEN. The waveforms are calculated using the subroutine FMPHL in programs WHAMPFS. The technique entails computing the complete theoretical amplitude spectrum as the product of the von Seggern-Blandford source spectrum, an attenuation operator $\exp(-\omega t^*/2)$ and the WWSSN long-period instrument response. The phase is calculated as the Hilbert transform of the log spectrum and the complete spectrum inverted to the time domain. The result is convolved in the time domain with delta functions to give the direct wave and pP as appropriate. For Figures 16a,b,c a reflection coefficient of -1.0 is assumed. Note that in Figure 16 this technique automatically yields an increasing time delay for first motion (as appropriate from causality considerations) as the yield and t* becomes larger.

To the left of each waveform in Figure 16 is plotted numbers for parameters derived by automatic processing. The period, T, is taken to be twice the time interval between the first peak and subsequent trough. In the case of no pP this assumption probably results in a period which is qualitatively too long. For the logarithm of the amplitude, log (A), the amplitude is taken from the same peak-to-trough excursion. For log (A/T), A is corrected for the WWSSN response at period T. The integral from 0.5 to 2.0 Hz is calculated by dividing the calculated amplitude spectrum by the WWSSN long-period system response, squaring the result, and integrating from 0.5 to 2.0 Hz. The result is the root-mean-square true ground displacement from 0.5 to 2.0 Hz. The number plotted is the logarithm of this number.

Appropriate waveforms for events in this study are indicated by event names next to the waveform. PILEDRIVER appears on two waveforms because its scaled delay time lies midway between .03 and .05. Note also that BOXCAR, BENHAM, GREELEY, JORUM, and HANDLEY all have similar source parameters and fall on the same waveform.

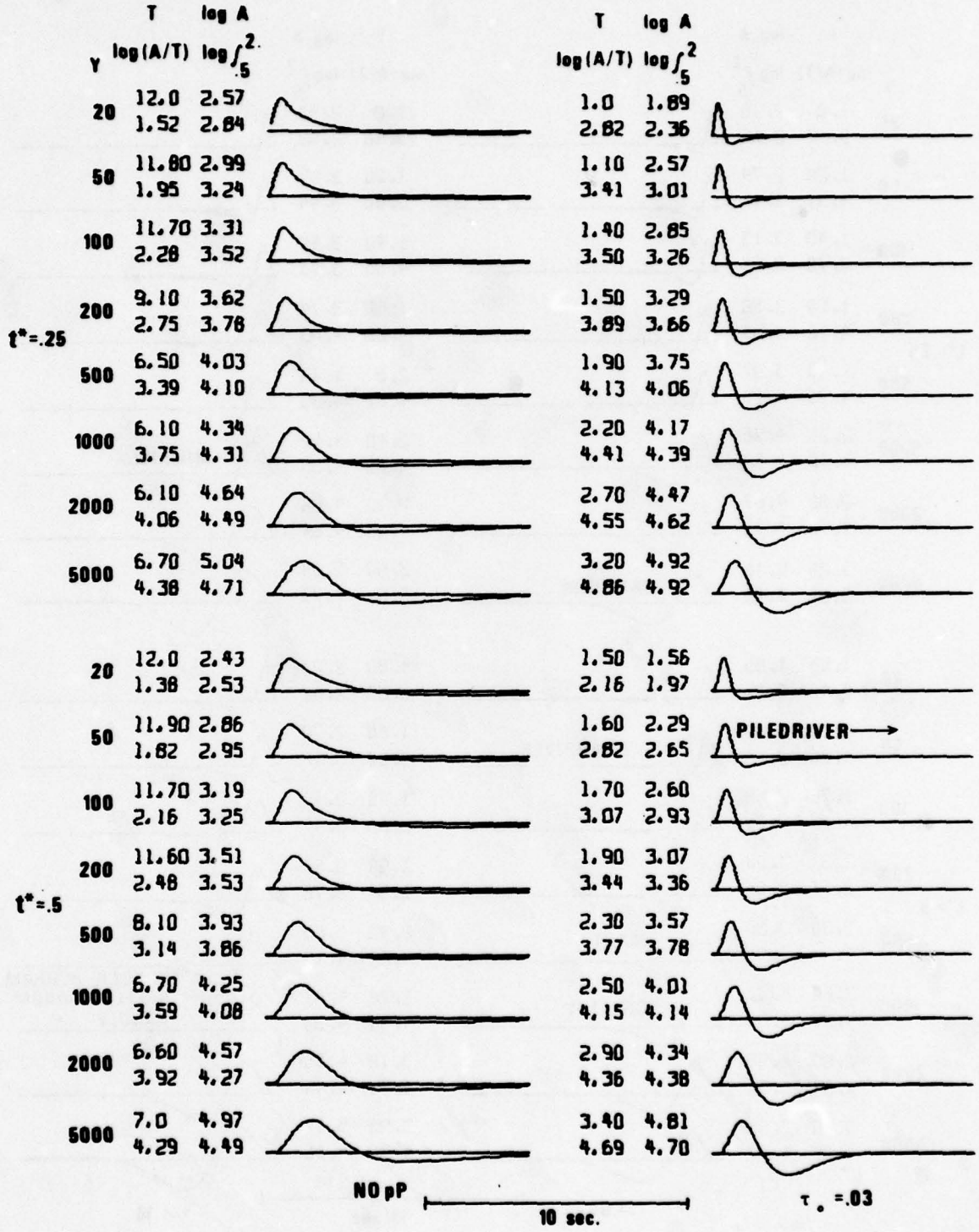

Figure 16a. WWSSN long-period theoretical waveforms for a granite reduced displacement potential, assuming perfect reflection for pP.

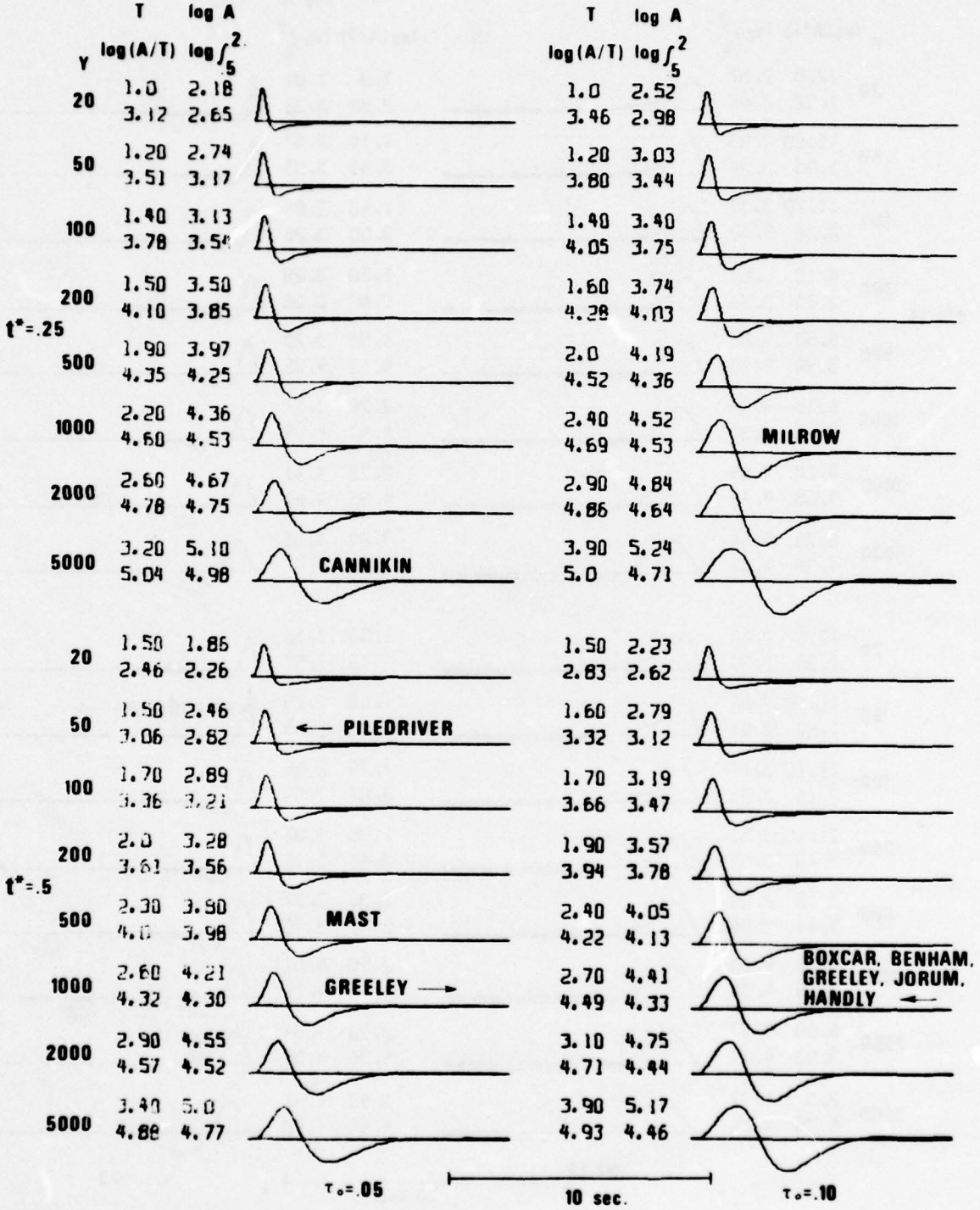

Figure 16b. WWSSN long-period theoretical waveforms for a granite reduced displacement potential, assuming perfect reflection for pP.

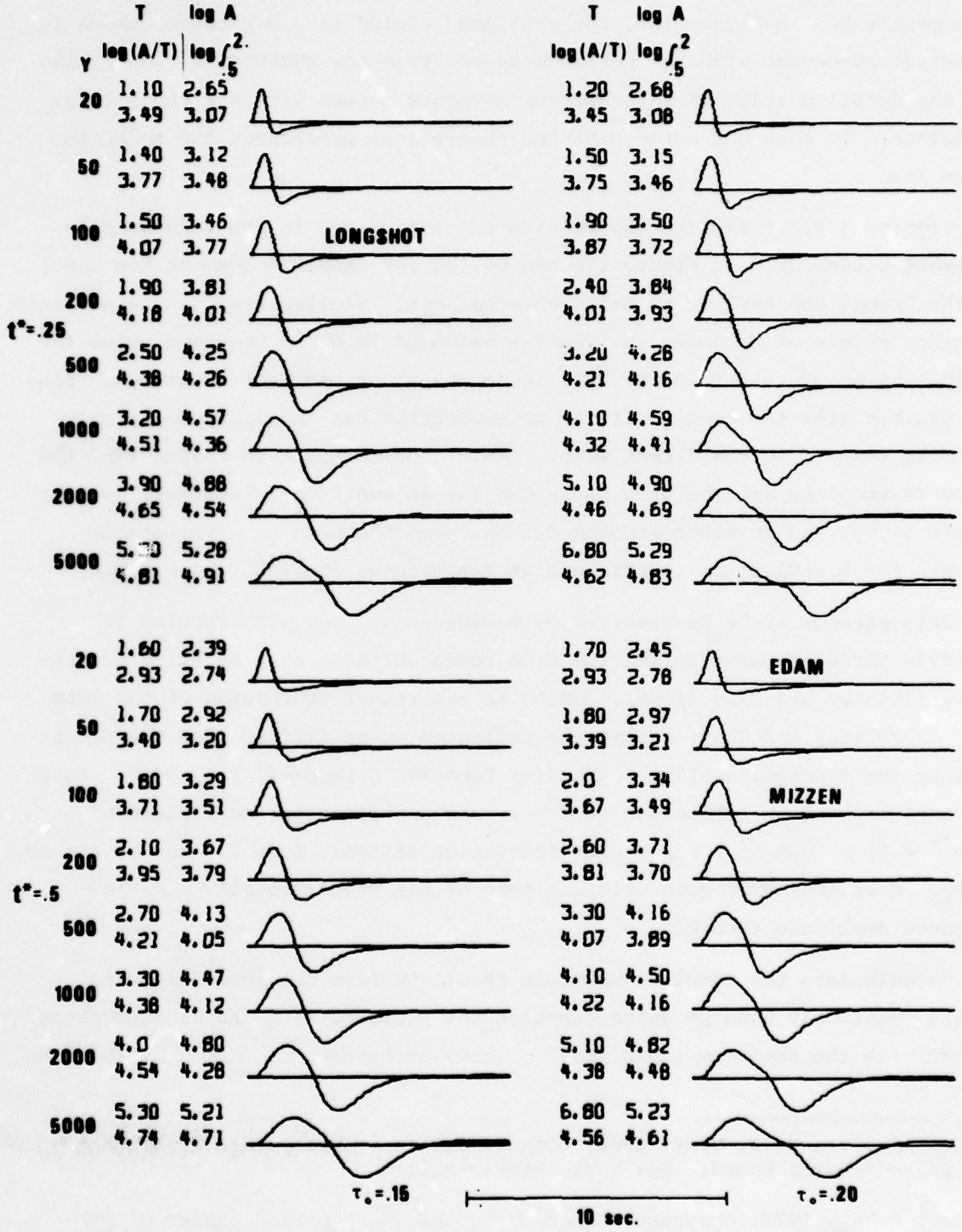

Figure 16c. WWSSN long-period theoretical waveforms for a granite reduced displacement potential, assuming perfect reflection for pP.

CANNIKIN provides the best data available for a comparison between theory and experiment. In Figure 16b, the predicted period is 3.2 seconds, which is in perfect agreement with the period measured from the WWSSN film. Note also that the detailed shape of the observed waveform agrees with the theoretical prediction. It does not agree with the theoretical prediction for no pP in Figure 16a.

Figures 17a,b,c explore the results of setting B=0 in the reduced displacement potential. In Figure 17b the period for CANNIKIN becomes too long, and the trough too shallow to match observations. Similar results are obtained for other values of k_o above the granite value of 16.8. A non-zero value for B, implying an overshoot in the RDP, is necessary to match observations. Figures 18a,b,c give the results if the pP reflection has an amplitude of only -0.5 with respect to the direct wave. Again, for CANNIKIN in Figure 18b, the period is too long and the trough has too low an amplitude. However, earlier in this study, and in other studies 0.5 has been shown to be a reasonable estimate for a reflection coefficient at frequencies above 0.5 to 1.0 Hz.

This paradox might be resolved by making an analogy with results in acoustics for plane wave reflection from rough surfaces as a function of frequency (Tolstoy and Clay (1966). Using an analytical expression of the form found in Tolstoy and Clay, assume the reflected pulse differs from the direct pulse by the spectral amplitude transfer function $0.5\exp(-f^2/f_r^2) + 0.5$. Note this implies perfect reflection at f = 0, and a reflection coefficient of $0.5(e^{-1} + 1) = 0.68$ at $f = f_r$. The transition is rapid from 1.0 to 0.5 around $f = f_r$. Frasier (1972) gave evidence that pP has proportionally more low-frequency amplitude than P.

To calculate the complete waveform resulting from the lower frequency pP, the previously used pP delta function was replaced with the minimum phase wavelet with the spectrum shown above. Then, as before, the initial "P" delta

---

Tolstoy, I., and C. I. Clay, 1966, Ocean Acoustics. Theory and Experiment in underwater sound: New York, McGraw-Hill.

Frasier, C. W., 1972, Observations of pP in the short-period phases of NTS explosions recorded at Norway; Geophys. J. R. Astr. Soc., 31, 99-109.

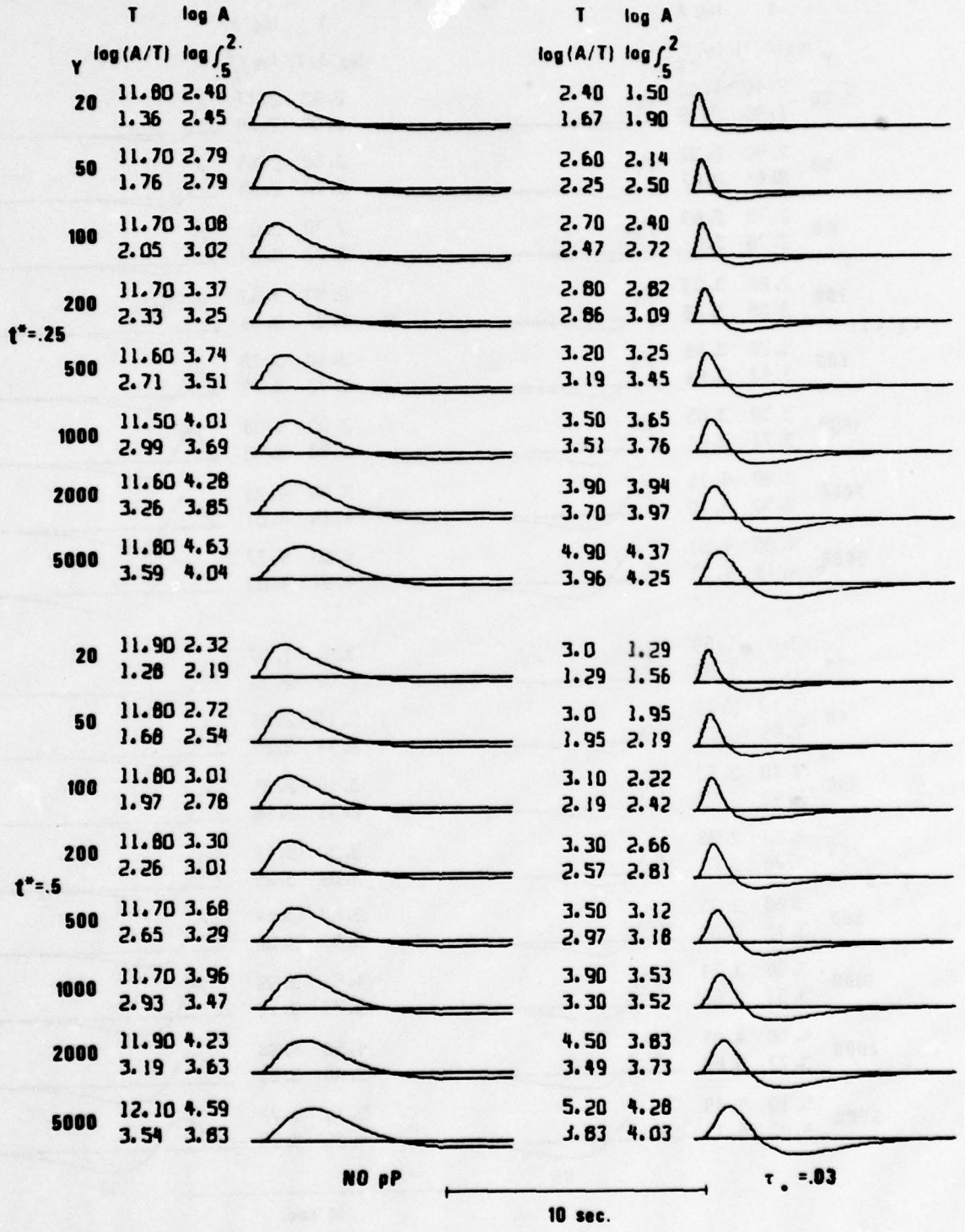

Figure 17a. WWSSN long-period theoretical waveforms for a granite reduced displacement potential modified by setting B=0, assuming perfect reflection for pP.

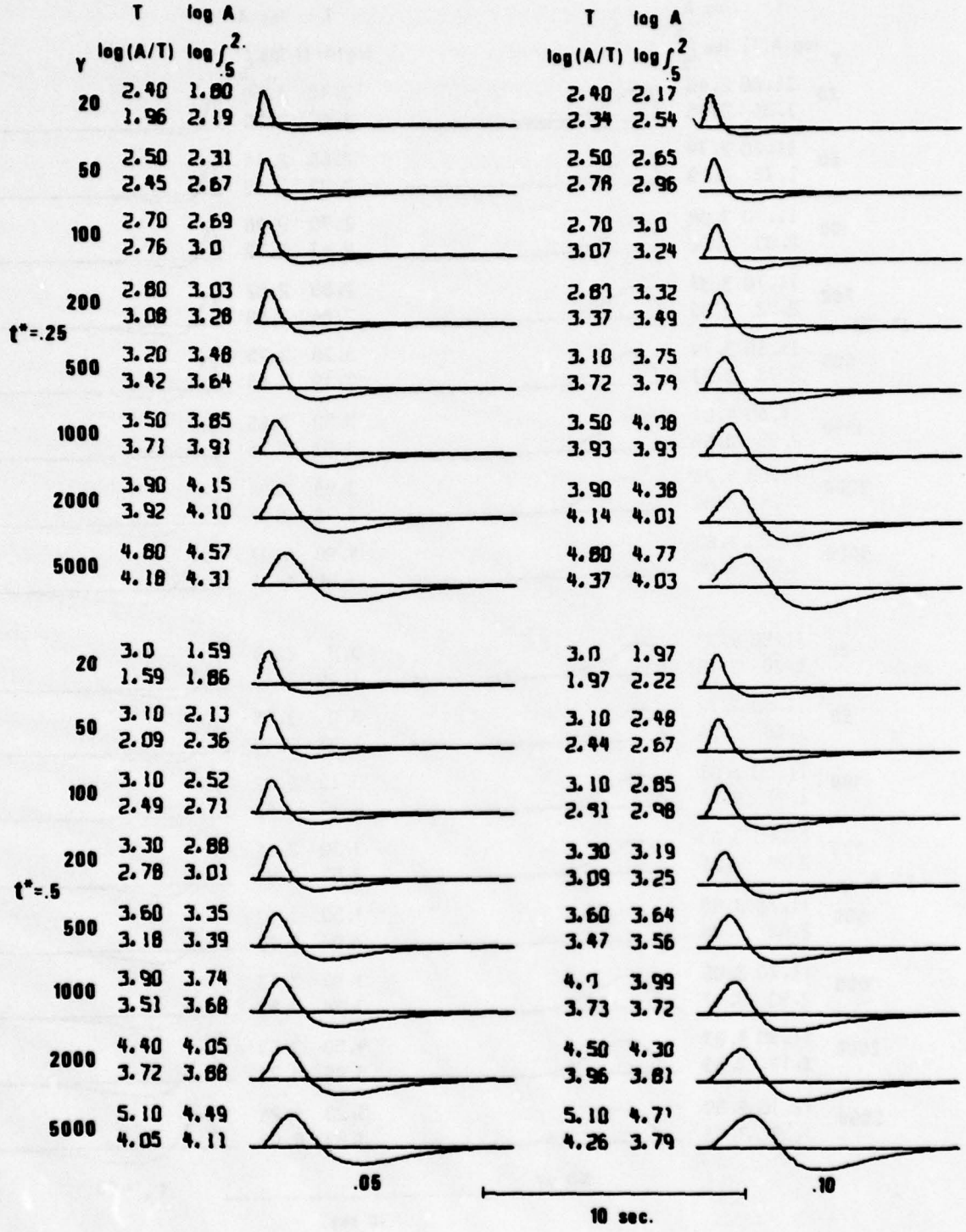

Figure 17b. WWSSN long-period theoretical waveforms for a granite reduced displacement potential modified by setting B=0, assuming perfect reflection for pP.

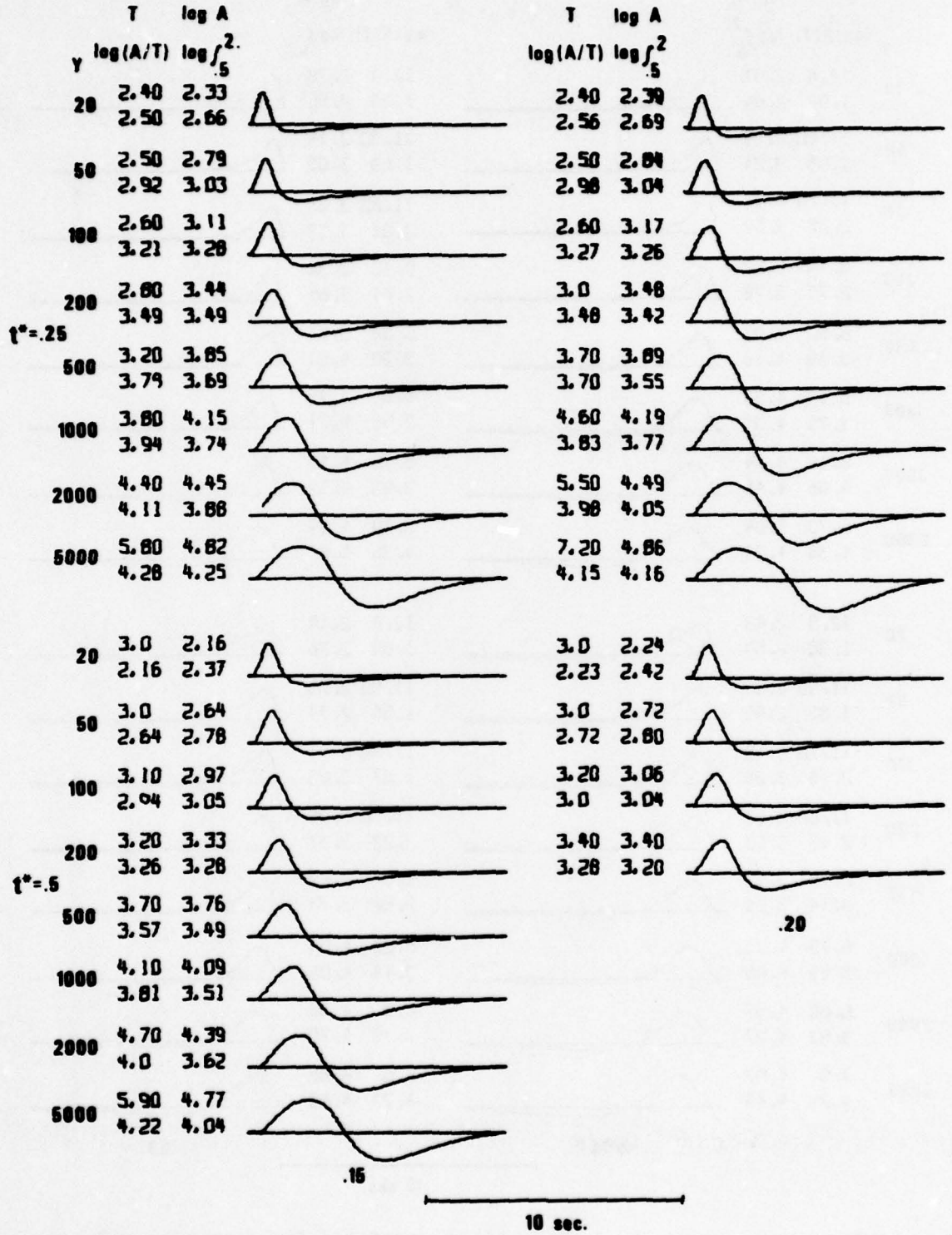

Figure 17c. WWSSN long-period theoretical waveforms for a granite reduced displacement potential modified by setting B=0, assuming perfect reflection for pP.

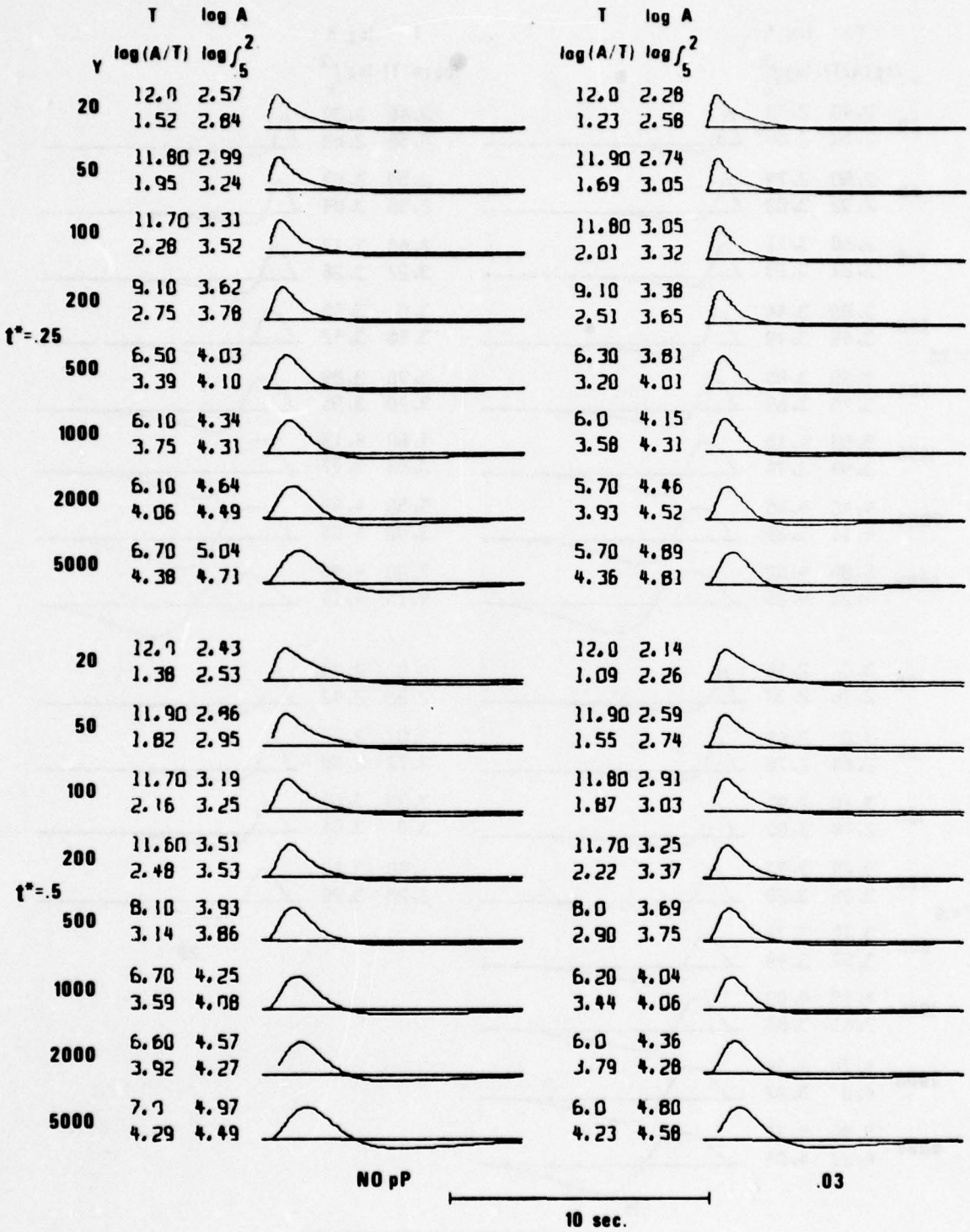

Figure 18a. WWSSN long-period theoretical waveforms for a granite reduced displacement potential. pP reflection coefficient is -0.5.

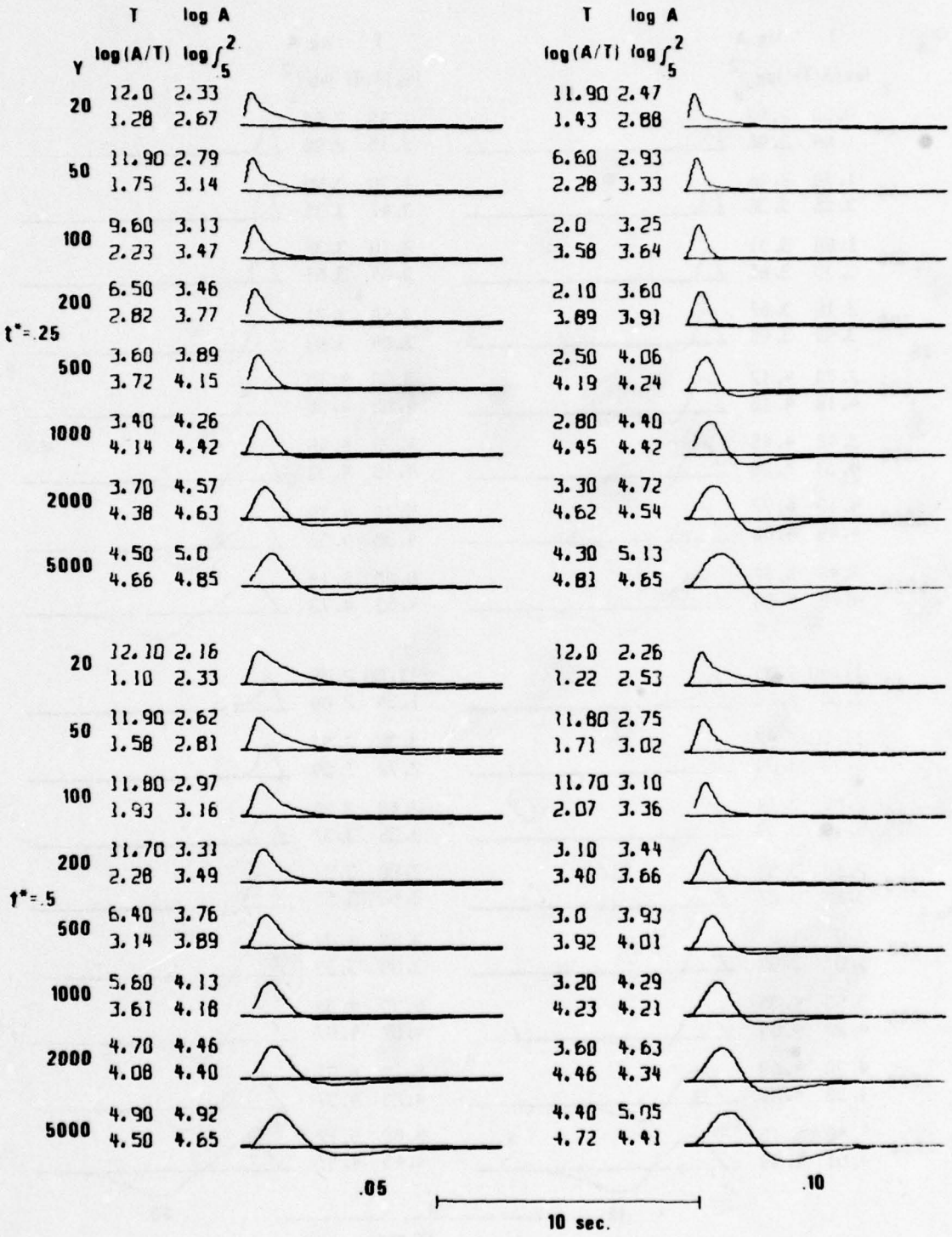

Figure 18b. WWSSN long-period theoretical waveforms for a granite reduced displacement potential. pP reflection coefficient is -0.5.

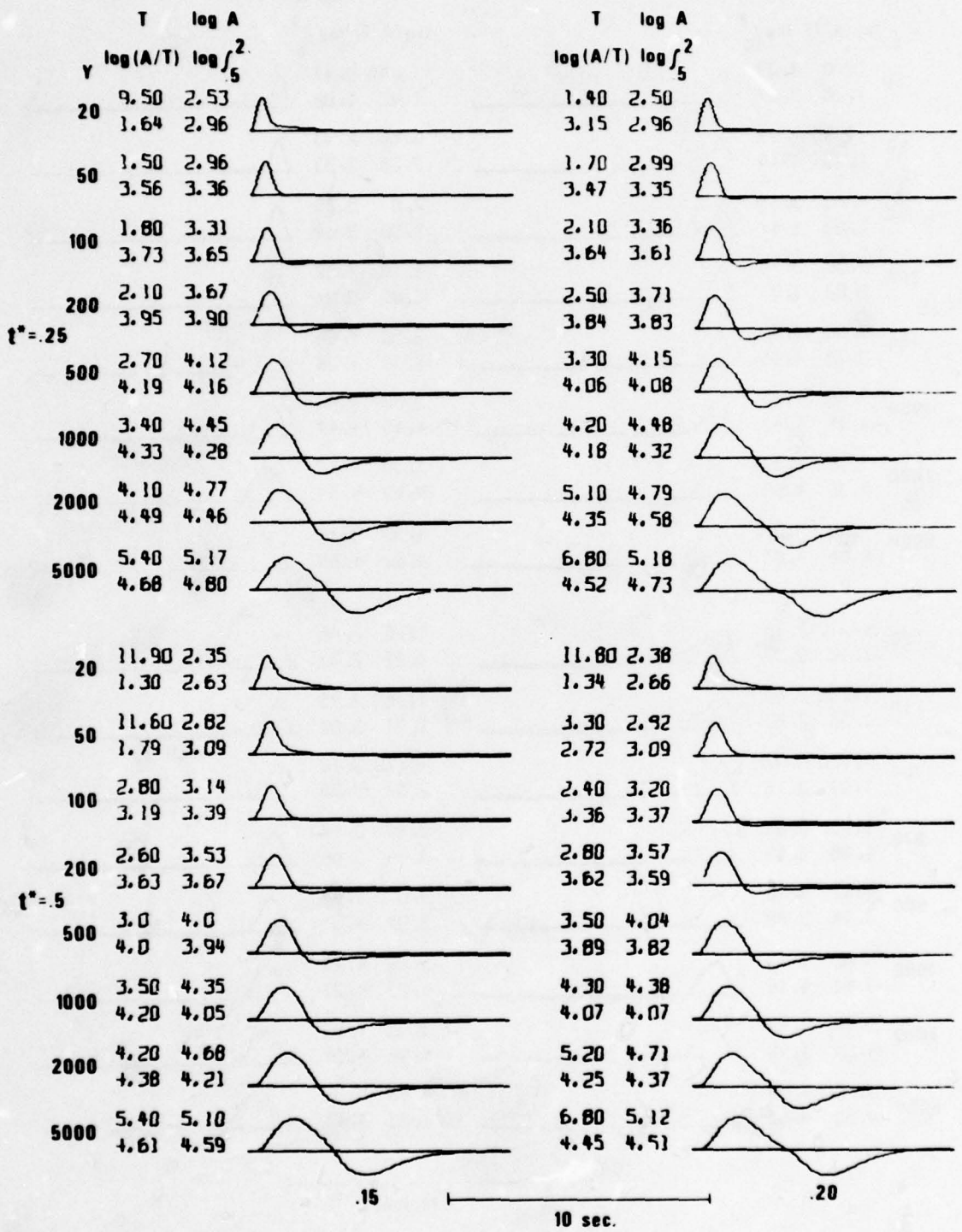

Figure 18c. WWSSN long-period theoretical waveforms for a granite reduced displacement potential. pP reflection coefficient is -0.5.

function plus this minimum phase wavelet appropriately delayed were convolved with the overall source mechanism-absorption-instrument response wavelet.

The results are seen in Figures 19a,b,c and 20a,b,c for f_r = 1.0 and 0.25 respectively. For CANNIKIN, perfect reflection existing only below f = 1.0 and perhaps only below 0.25 gives satisfactory agreement with observations. Even with f_r = 0.25, agreement is much better with Figure 16 where the reflection coefficient is -1.0 than with Figure 18 where it is -.5. This analysis strongly suggests that the reflection coefficient for pP from CANNIKIN is close to 1.0 for frequencies somewhere below 1.0 Hz.

Adequately hand-digitizing high-frequency signals from explosions on long-period records is difficult. For this reason, attempts were made to transform the LRSM signals of explosions studied in this report into the form they would have had if they were recorded on a WWSSN long-period system. To do this we divided the complex observed signal spectrum by the complex LRSM response, and then multiplied it by the complex WWSSN response. In practice, the system phase responses are determined from their log amplitude responses by means of the discrete Hilbert transform. This process is applied only to the vertical components, and only at those stations for which, after deconvolution, there seems to be a detectable long-period signal. The signals were aligned using the start of the short-period signal. The summed results are shown in Figure 21. Periods of resulting signals have been measured and are compared to the theoretical values in Table III, which also includes a small plot of the period data. While the agreement is good, there seems to be a general bias: the observed periods after deconvolution are shorter than those theoretically predicted.

Significantly, in this respect, the deconvolved period for CANNIKIN is 2.5 seconds, compared to the 3.2 seconds, observed directly from the film which agreed with theory. Perhaps there is some effect of the large long-period noise level (most of which is probably LRSM system noise) in the deconvolved data that shortens the observed period. Experiments using the high dynamic range SRO stations may resolve this question.

Contours of log(A) and T as function of yield and τ_o are drawn in Figure 22 for t* = 0.25 sec and 0.5 sec. The values contoured are taken from Figure 16, the granite parameters with perfect reflection. Note that for

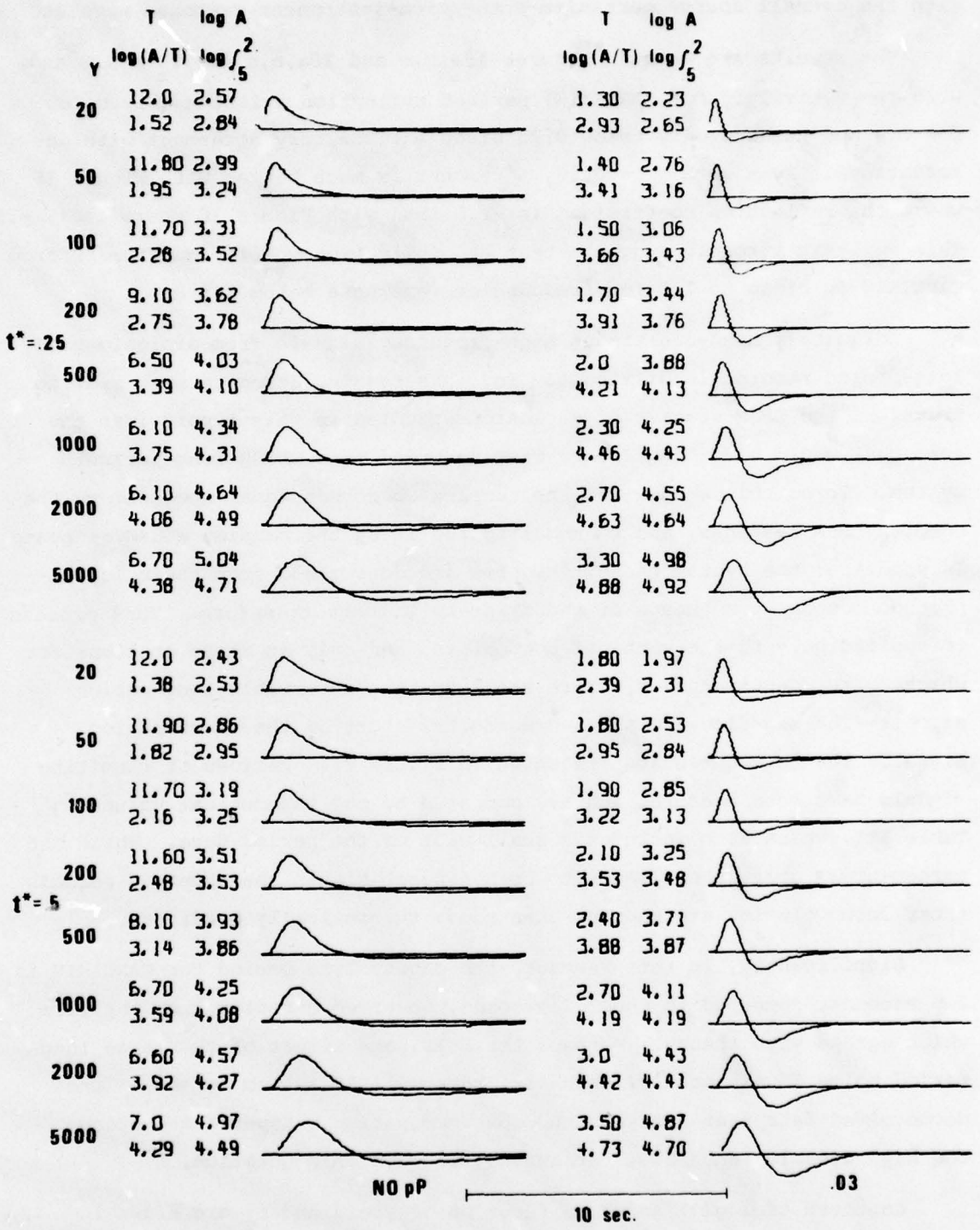

Figure 19a. WWSSN long-period theoretical waveforms for a granite reduced displacement potential, pP reflection coefficient varies according to $0.5\exp(-f^2/1.) + 0.5$.

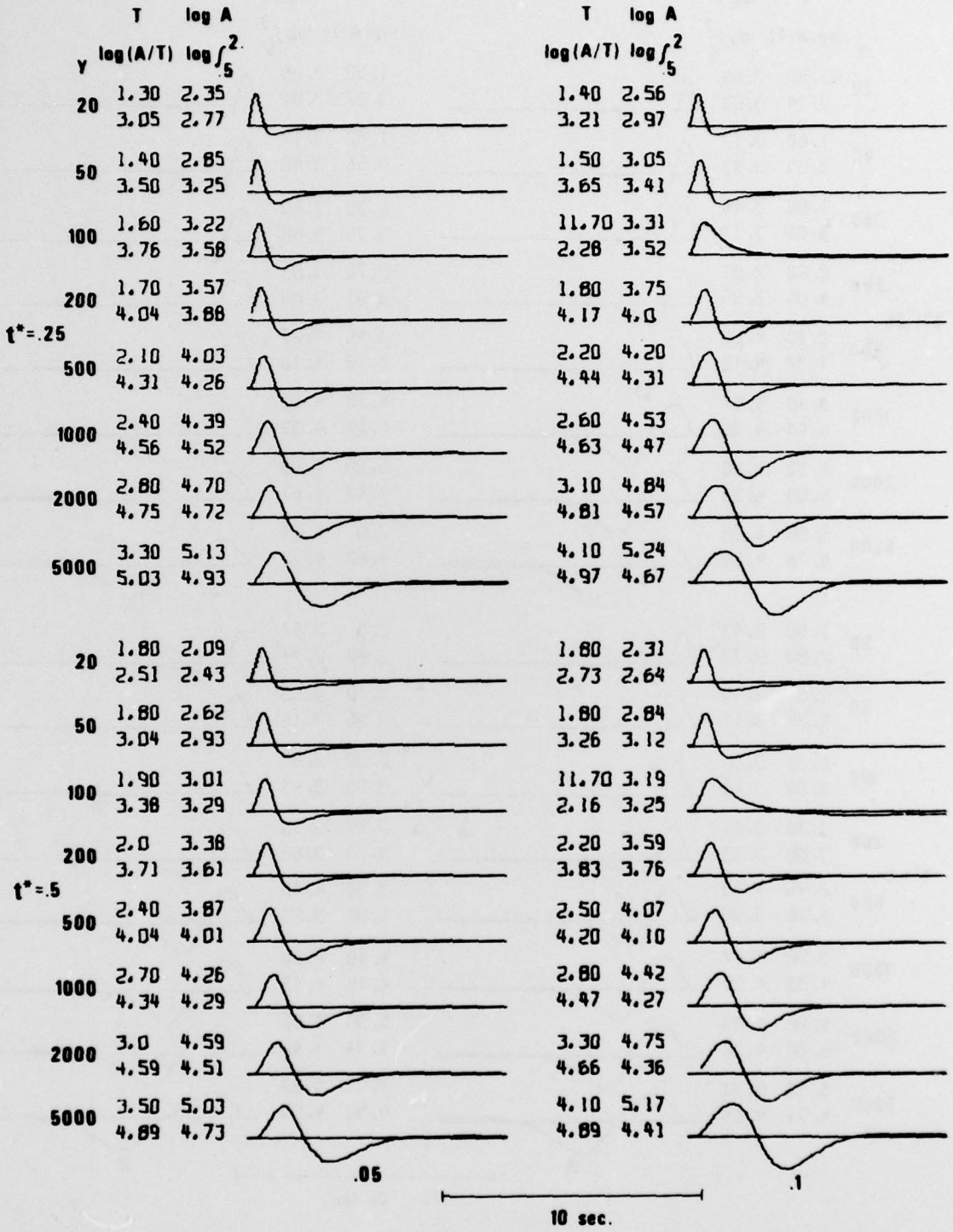

Figure 19b. WWSSN long-period theoretifal waveforms for a granite reduced displacement potential, pP reflection coefficient varies according to $0.5\exp(-f^2/1.) +0.5$.

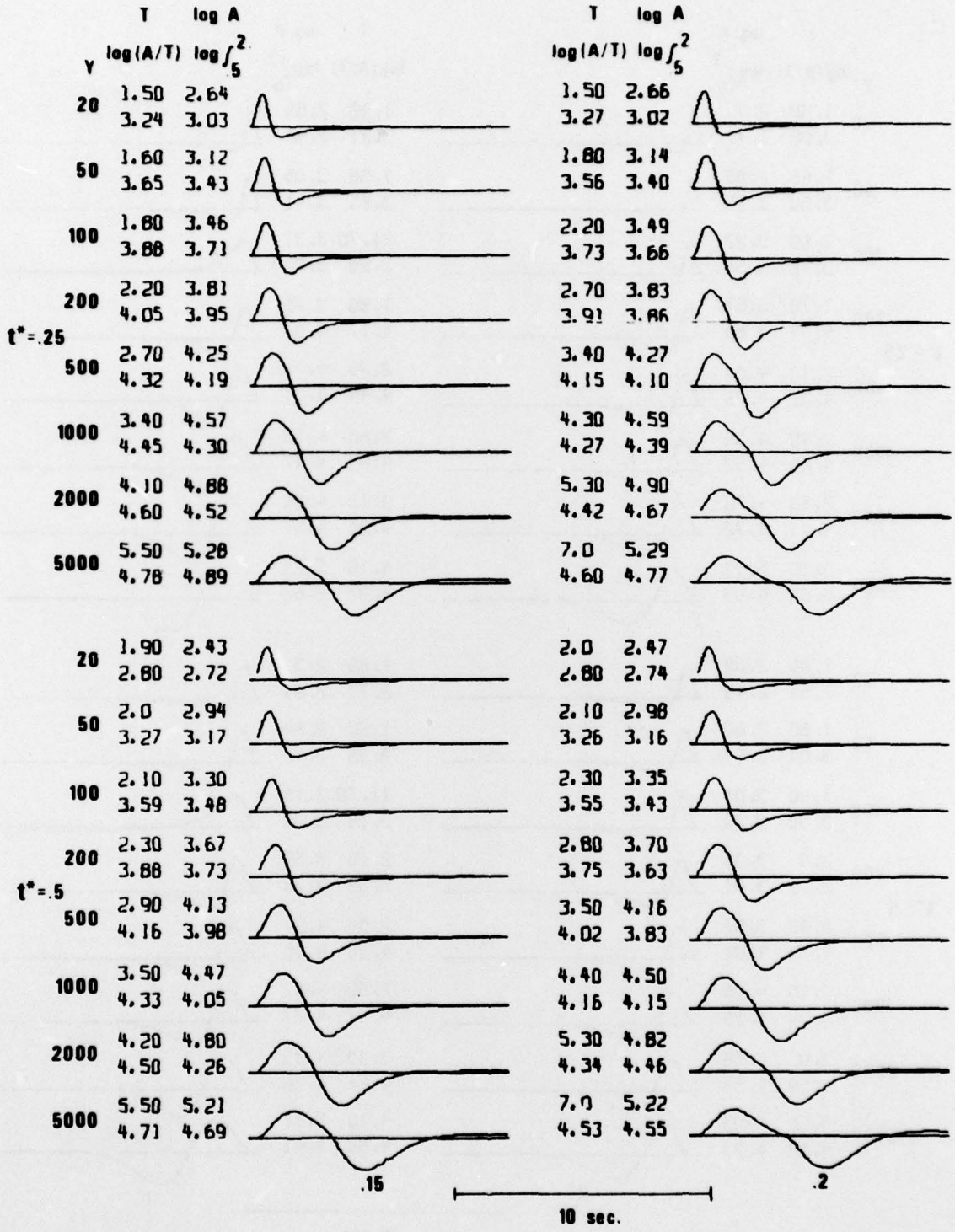

Figure 19c. WWSSN long-period theoretical waveforms for a granite reduced displacement potential, pP reflection coefficient varies according to $0.5\exp(-f^2/1.) + 0.5$.

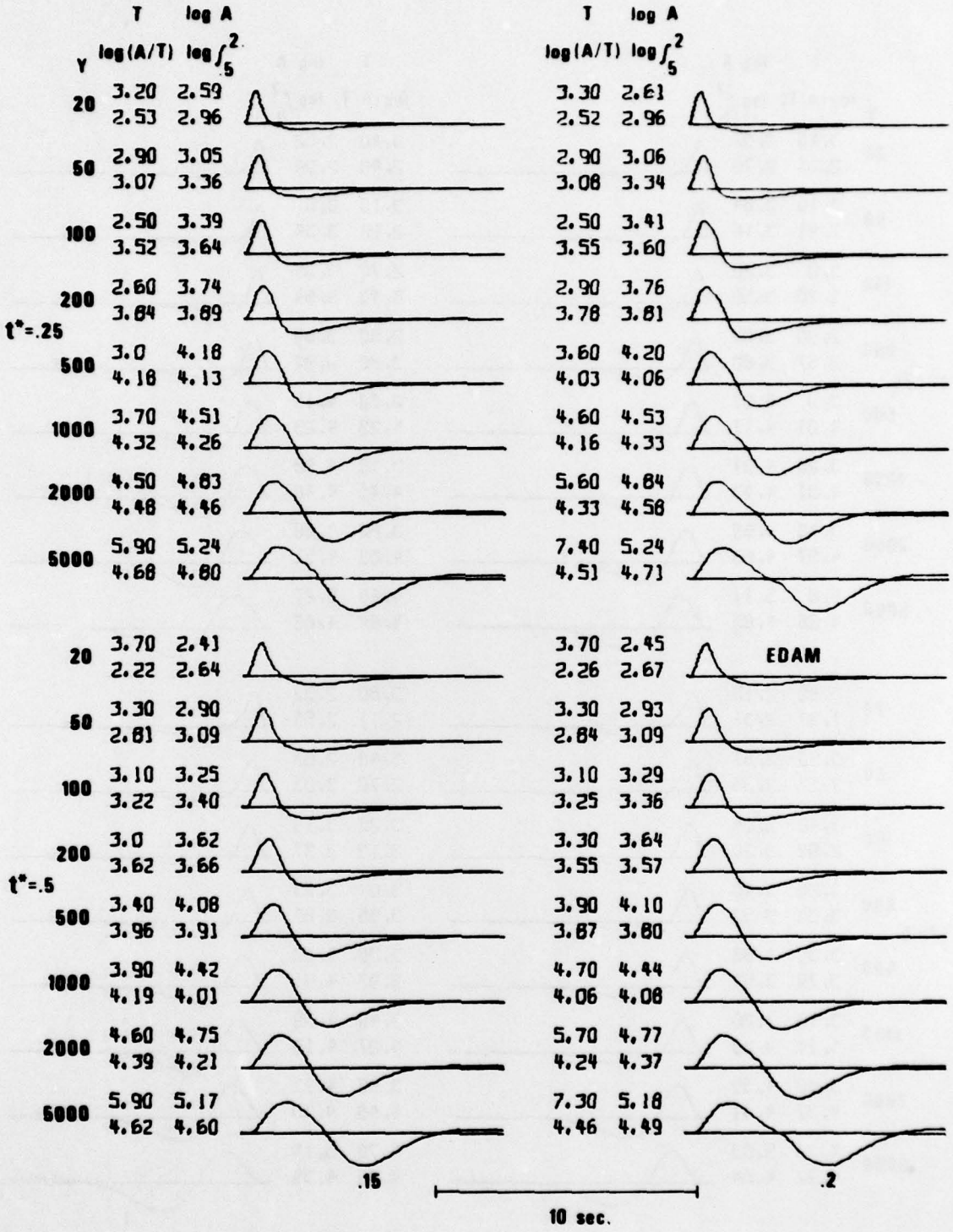

Figure 20a. WWSSN long-period theoretical waveforms for a granite reduced displacement potential, pP_2 reflection coefficient varies according to $0.5\exp(-f^2/.25^2) + 0.5$.

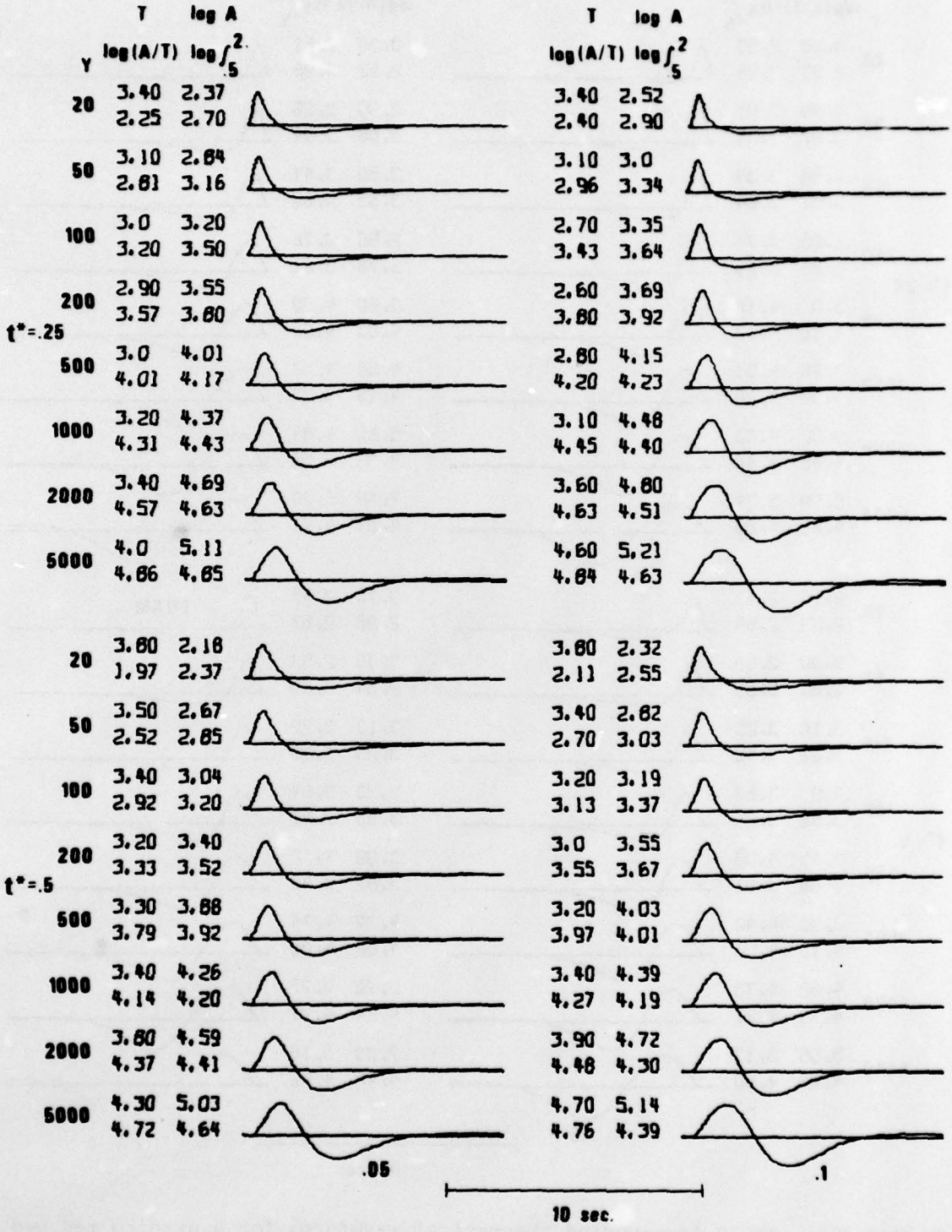

Figure 20b. WWSSN long-period theoretical waveforms for a granite reduced displacement potential, pP_2 reflection coefficient varies according to $0.5\exp(-f^2/.25^2) + 0.5$.

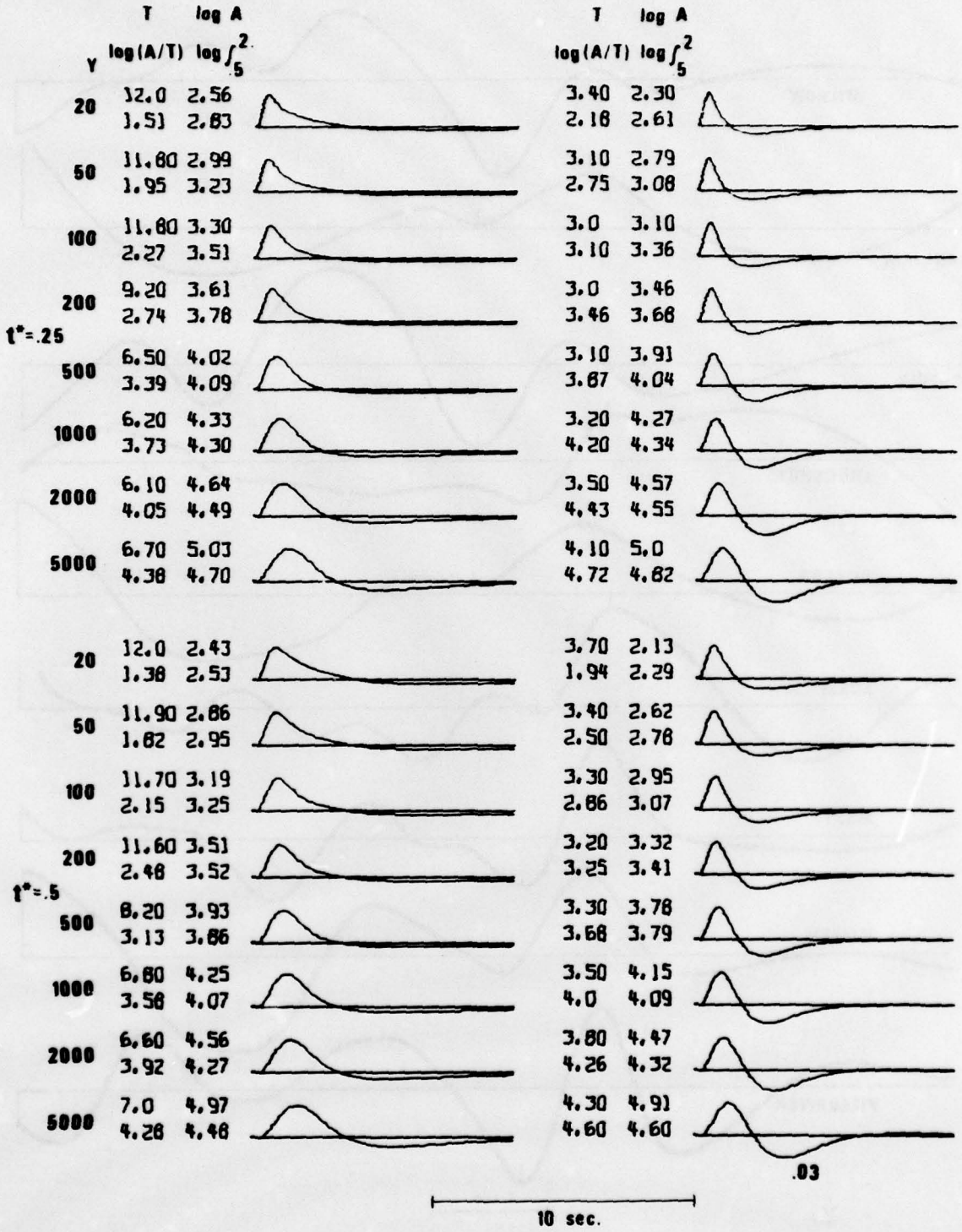

Figure 20c. WWSSN long-period theoretical waveforms for a granite reduced displacement potential, pP_2 reflection coefficient varies according to $0.5\exp(-f^2/.25^2) + 0.5$.

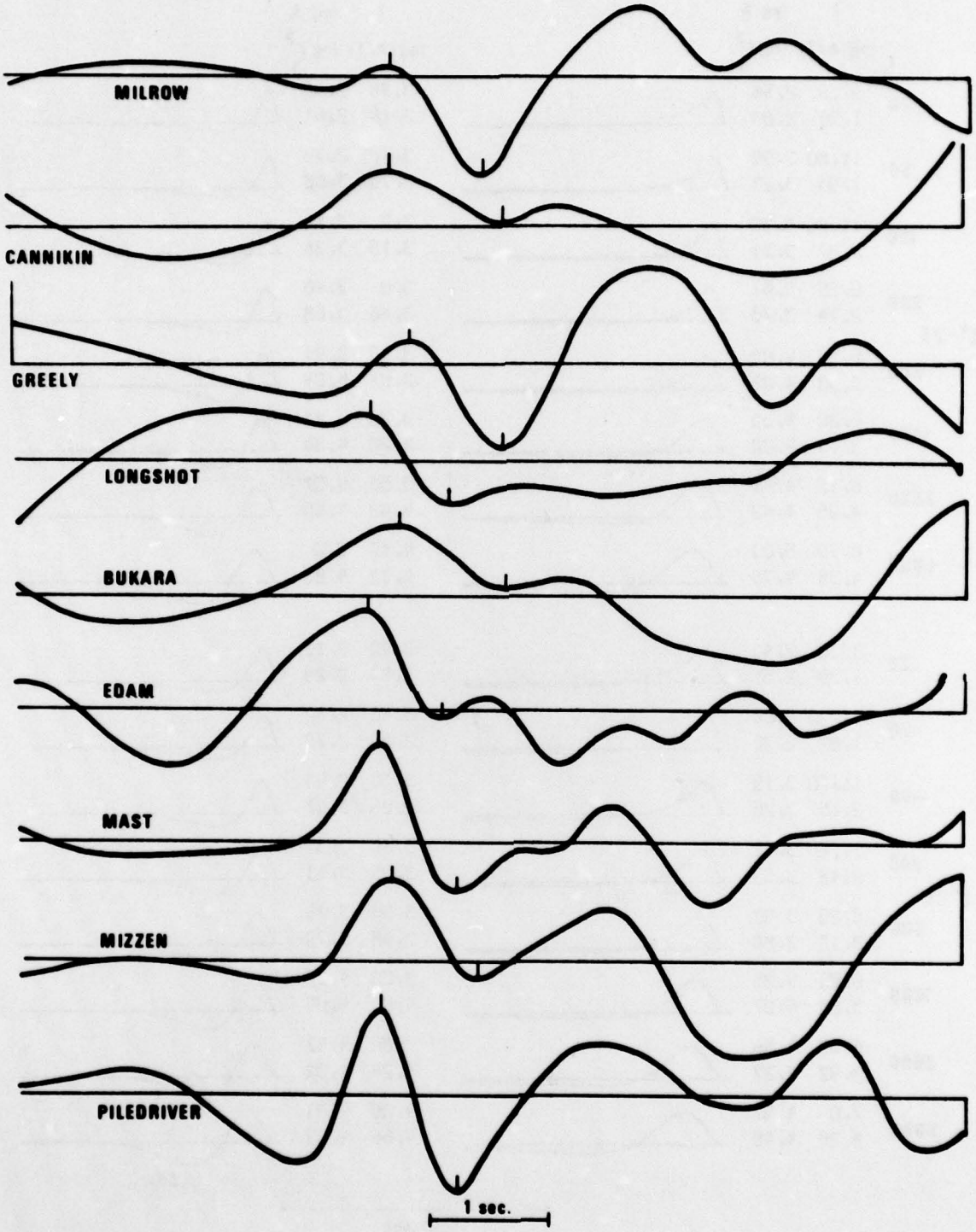

Figure 21. LRSM short-period vertical recordings transformed to the appearance they would have on WWSSN long-period systems, aligned on the short-period arrival times and summed over the network. One sum trace is presented for each event in the report.

TABLE III

Maximum-likelihood delays, together with the theoretical WWSSN long-period measured periods which explosions with those pP delay and appropriate yields would produce. These are compared with the observed periods taken from deconvolved LRSM records except for the case of CANNIKIN where an average directly measured period is also reported. Also for CANNIKIN we have used $\tau = 1.0$ instead of the calculated 0.55.

	τ_{pP} MAX -LIKE	THEORETICAL B=2 k_o=16.8	OBSERVED
MILROW	.85	2.4	1.9
CANNIKIN	.55	3.2	2.5 (3.2, film)
GREELEY	.70	2.6	1.9
LONGSHOT	.55	1.5	1.7
BUKARA	1.2	not calculated	2.2
EDAM	.55	1.7	1.5
MAST	.50	2.3	1.7
MIZZEN	.95	2.0	1.8
PILEDRIVER	.15	1.6	1.6

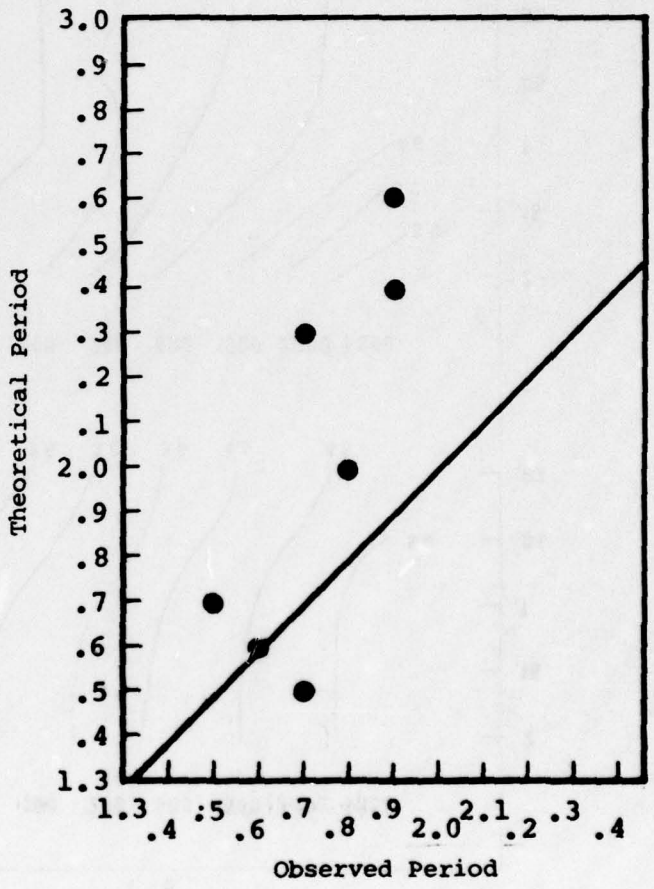

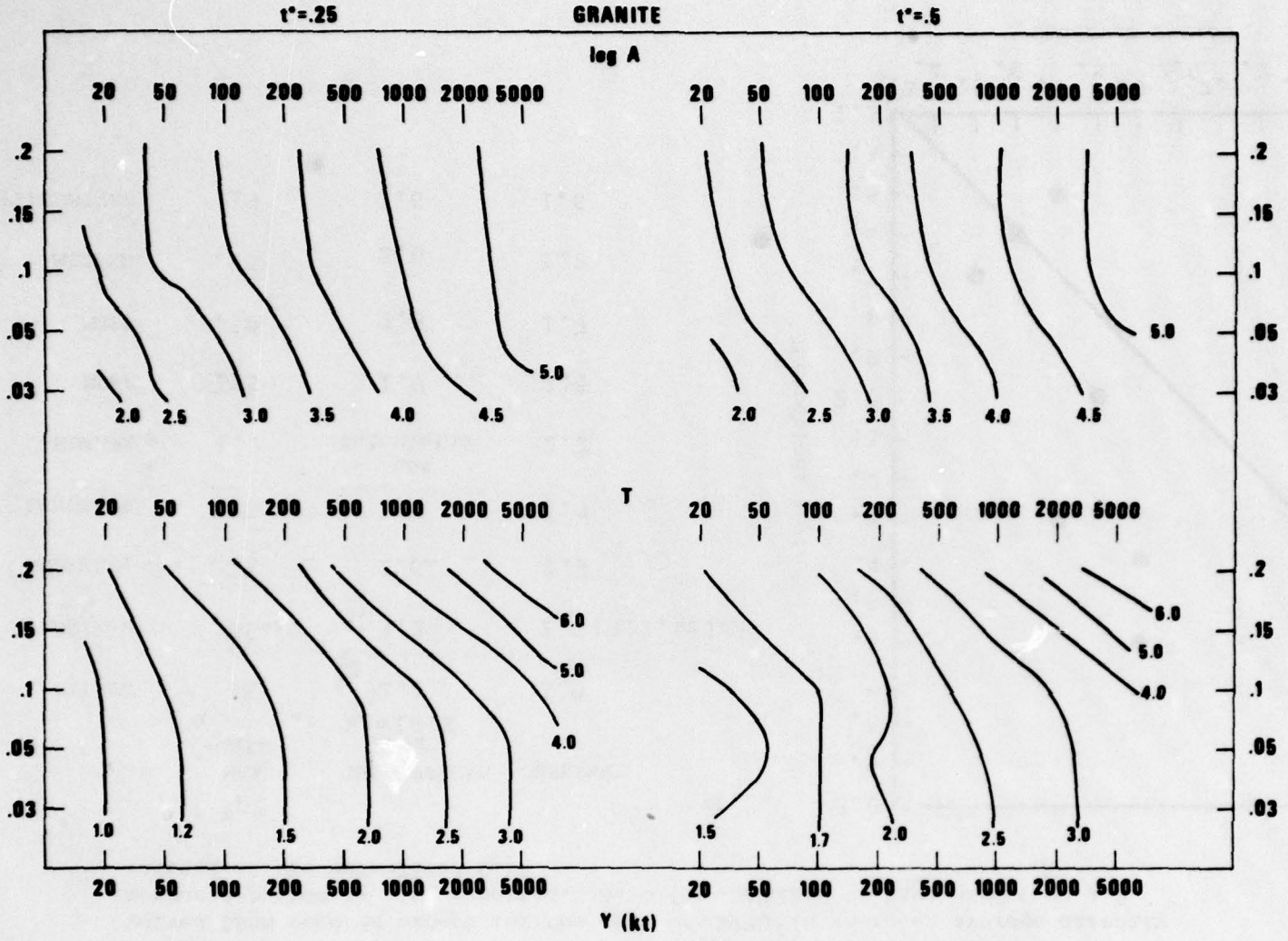

Figure 22. Amplitude and period of theoretical WWSSN long-period waveforms with perfect pP reflection (from Figure 4) contoured as a function of yield and τ_o for two values of t*. Non-parallelism of the contours shows that in theory delay and yield may be determined from amplitude and period.

fixed t* the families of contours are generally not parallel so that specification of an amplitude and a period will determine yield, and τ_p and, therefore, the pP delay. The amplitude graph for t* = 0.25 could be calibrated by CANNIKIN, and for t* = 0.5, JORUM or some other large NTS shot. Clearly, however, the reduced displacement potential must be known a-priori to be satisfactory for the test site under consideration.

This technique would be difficult to apply at present because of the poor time resolution and signal-to-noise ratio on WWSSN long-period traces. These problems may possibly be overcome to some degree by deconvolved SRO data, and by arrays to which multi-channel filtering may be applied to reduce the low-frequency noise.

CONCLUSIONS AND SUGGESTIONS FOR FURTHER RESEARCH

In conclusion, if the parameters of the source signal spectrum are specified correctly, then the time delays and amplitudes for a single reflection can be estimated by maximum likelihood. Difficulties exist in specifying the initial values for the parameters B, C and t*. However, this could be accomplished by searching the likelihood over B, C and t* but in results not reported here this has yielded unreasonable values for these parameters. The problem of estimating the source spectrum for BUKARA was, however, satisfactorily solved in this report by an heuristic iterative approach.

Another potential problem is the presence of multiple arrivals when the model is essentially a single reflection spectrum. In the simulated example presented here this seemed to be a less important problem as the single reflection likelihood function successfully resolved a double reflection example.

Nonetheless perhaps another approach to the multiple arrival problem should be tried. Conceivably, this was the difficulty with CANNIKIN because five separate arrivals of high likelihood were detected and the single arrival model may be inadequate in so complex a situation. Research also seems warranted on the problem of distinguishing precursors from later multipaths.

Another source of difficulties with CANNIKIN could be that the pP reflection coefficient is varying with frequency through the dominant part of the signal spectrum. This variation violates the hypothesized model of a constant reflection coefficient. Research could be carried out with a more satisfactory model to determine if this problem with CANNIKIN can be solved.

Various informal attempts have been made to estimate the stability of the results to the a-priori estimates of B, C, and t*. In general variations of 20 to 30% in these parameters do not significantly change the final results. Still, however, a more complete investigation of this question seems warranted.

Finally, the most promising result in this study is the successful determination of the delay for PILEDRIVER. This effort is of great importance because many of the explosions in the USSR are apparently detonated in high-velocity media, and detonated at depths where the delay time is very short. The maximum-likelihood technique should, therefore, be tried out on

more events with short-delay times, such as USSR shots, and small NTS shots. The NTS shots might have to be analyzed using data from fairly close LRSM stations.

REFERENCES

Bakun, W. H. and L. R. Johnson (1973). The deconvolution of teleseismic P waves from explosions MILROW and CANNIKIN, Geophys, J. R., Astr. Soc. 34, 321-342.

Bogert, B. P., M. J. R. Healy, and J. W. Tukey (1962). The frequency analysis of time series for echoes: ceptrum, pseudo-autocovariance, cross ceptrum and phase cracking, in Proc. on Time Series Analysis, ed. M. Rosenblatt, John Wiley and Sons, New York.

Cohen, T. J. (1970). Source-depth determinations using spectral pseudo-autocorrelation and ceptral analysis, Geophys. J. R. Astr. Soc., 20, 223-231.

Cohen, T. J. (1975). P_s and pP phases from seven Pahute Mesa events, Bulletin of the Seismological Society of America, 65(4), 1029-1032.

Der, Z. A. and T. W. McElfresh (1976). The effect of attenuation on the spectra of P waves from nuclear explosions in North America, SDAC-TR-76-7, Teledyne Geotech, Alexandria, Virginia. ADA 030857

Douglas, A., P. J. Corbishley, C. Blamey, and P. D. Marshall (1972). Estimating the firing depth of underground explosions, Letters to Nature, 237, 26-28.

Flinn, E. A., T. J. Cohen, and D. W. McCowan (1973). Detection and analysis of multiple seismic events, Bull. Seism. Soc. Am., 63(6), 1921-1936.

Frasier, D. W. (1972). Observations of pP in the short-period phases of NTS explosions recorded at Norway, Geophys. J. R. Astr. Soc., 31, 99-109.

Hannan, E. J. and P. J. Thomson (1974). Estimating echo times, Technometrics, 16(1), 77-84.

Hasegawa, H. S. (1971). Analysis of teleseismic signals from underground nuclear explosions originating in four geological environments, Geophys. J. R. Astr. Soc., 24, 365-381.

Marshall, P. D. (1972). Some seismic results from a world wide sample of large underground explosions, AWRE Report 0 49/72, Atomic Weapons Research Establishment, Aldermaston, Berkshire, United Kingdom.

Orphal, D. L., C. T. Spiker, L. R. West, and M. D. Wronski (1970). Analysis of seismic data MILROW event, Environmental Research Corporation, Alexandria, Virginia NVO-1163-209.

Springer, D. L. (1974). Secondary sources of seismic waves from underground nuclear explosions, Bull. Seism. Soc. Am., 64, 581-594.

Tolstoy, I. and C. I. Clay (1966). Ocean acoustics, theory and experiment in underwater sound: New York, McGraw-Hill, 293.

von Seggern, D. and R. Blandford (1972). Source time functions and spectra for underground nuclear explosions, Geophys. J. R. Astr. Soc., 31, 83-97.

Wyss, M. and T. C. Hanks (1972). The source parameters of the San Fernando earthquake inferred from teleseismic body waves, Bull. Seism. Soc. Am., 62, 591-602.